

2020-10-26

Sampling Using Controlled Quantum Walks

Bencivenga, Dante

Bencivenga, D. (2020). Sampling Using Controlled Quantum Walks (Master's thesis, University of Calgary, Calgary, Canada). Retrieved from <https://prism.ucalgary.ca>.

<http://hdl.handle.net/1880/114117>

Downloaded from PRISM Repository, University of Calgary

UNIVERSITY OF CALGARY

Sampling Using Controlled Quantum Walks

by

Dante Bencivenga

A THESIS

SUBMITTED TO THE FACULTY OF GRADUATE STUDIES
IN PARTIAL FULFILLMENT OF THE REQUIREMENTS FOR THE
DEGREE OF MASTER OF SCIENCE

GRADUATE PROGRAM IN COMPUTER SCIENCE

CALGARY, ALBERTA

OCTOBER, 2020

© Dante Bencivenga 2020

Abstract

We give a new quantum algorithm to sample from probability distributions over graph vertices quadratically faster than the optimal classical algorithm, which uses random walks with stopping rules. Efficient sampling is an important computational task used in simulations based on stochastic processes. This is the first quantum algorithm that achieves a quadratic speed-up for sampling from general probability distributions over graph vertices.

Our algorithm generalizes the controlled quantum walk algorithm proposed by Dohtar and Høyer in 2015. Our main technical innovation is to allow for multiple distinct controlled reflections. This allows us to generate the quantum state analogous to the target probability distribution over vertices. This quantum state, when measured, gives a corresponding classical sample from the target distribution.

We also give a second classical algorithm for sampling from probability distributions over graph vertices. This algorithm adds different self-loops to each vertex of the random walk. We show how to construct the quantum analogue of this algorithm. Finally, we show that we can embed this quantum analogue into our controlled quantum walk.

Preface

The result presented in this thesis will be part of a manuscript written in collaboration between fellow student Xining Chen, my supervisor Peter Høyer, and myself.

Xining Chen's contribution was to prove that when the target distribution $\vec{\tau}$ corresponds to the distribution from an absorbing stopping rule (i.e. where we always stop in marked vertices) then $U(\vec{\theta})$ generates $|\tau\rangle$ quadratically faster than the classical hitting time by starting in $|0, \overline{\text{init}}\rangle$. I generalized this to any target distribution, and the speed-up is then over the access time, a generalization of the hitting time.

Acknowledgements

Research isn't a straight line from problem to solution. It's a series of twists and turns, of promising avenues that lead to dead ends, and, every once in a while, of new gems of knowledge that make the effort worth it. Us researchers are constantly working on problems that no one has solved before, and trying to reach a deeper understanding than anyone has ever reached. We're able to do this because we lean on each other.

My journey in the quantum walks research group spanned four years and involved collaborating with fantastic people. Thank you to my supervisor, Dr. Peter Høyer, for inspiring me to delve deeper into the world of algorithms, and for constantly pushing me further. Your passion for making the group constantly seek to improve as well as to strive for and reach new goals has helped us grow as scientists and as people.

When I joined the group, Cătălin Dohotaru, Alireza Poostindouz, Mojtaba Komeili, Arta Seify, and Jonathan Shabash welcomed me as we worked together to investigate new questions about quantum walks. Xining Chen then joined, and her enthusiasm for research laid the groundwork for the project that became my thesis. Over the years, I also had the pleasure to work with Spencer Wilson, Zhan Yu, Shang Li, Kyle Ostrander, Janet Leahy, and Elliot Evans as they contributed new perspectives to the group. Being friends with you has been an amazing part of my life, and I'm so grateful to have been a part of yours.

I am also deeply grateful to Dr. Philipp Woelfel and Dr. David Feder, who along with Peter examined this thesis. While preparing for a unique fall semester of teaching, you also took the time to improve my contribution to the field.

Lastly, I would like to thank my family, and especially my parents. You are there for me through the good times and the bad, and have done so much to help me be able to reach this accomplishment.

Table of Contents

Abstract	ii
Preface	iii
Acknowledgements	iv
Table of Contents	v
List of Figures	vi
1 Introduction	1
1.1 Sampling	1
1.1.1 Rejection Sampling	2
1.2 Random Walks	2
1.2.1 Stationary Distribution	3
1.2.2 Special Properties of Random Walks	4
1.2.3 Edge Weights of Reversible Walks	5
1.2.4 Discriminant Matrix	6
1.3 Quantum Walks	7
2 Sampling Using Random Walks with Stopping Rules	9
2.1 Access Time	9
2.2 Exit Frequencies	10
2.3 Local Stopping Rules	11
3 Quantum Walks	13
3.1 Quantum States and Operators	13
3.2 Quantum Hitting Time	14
3.3 Construction of Quantum Walks	15
3.3.1 Szegedy's Correspondence	17
3.4 Detecting and Finding	18
4 Controlled Quantum Walks	20
4.1 Construction	20
4.2 Stationary Eigenvector	21
5 Quadratic Speed-Up Over Access Time	23
5.1 Starting in $ \text{init}\rangle$	23
5.1.1 Quantum Rejection Sampling	28
5.2 Starting in $ \overline{\text{init}}\rangle$	30
6 Interpolated Walks	36
6.1 Construction	36
6.2 Sampling From Interpolated Walks	37
6.3 Embedding Quantum Interpolated Walks Into Controlled Quantum Walks	38
6.4 Extended Hitting Time	41
7 Conclusion	42
Bibliography	44
A Proof of the Flip-Flop Lemma	48
B General Real Unitaries	51

List of Figures

3.1	The quantum walk as the set of reflections about $ i, p_i\rangle$ followed by SWAP .	16
4.1	The circuit $U(\vec{\theta})$	21

Chapter 1

Introduction

In this chapter, we introduce the classical (i.e. non-quantum) concepts of sampling and random walks, and we introduce quantum walks. In Chapter 2, we combine the two classical concepts to introduce stopping rules of a random walk, which we use to sample from a target probability distribution over vertices. In Chapter 3, we introduce quantum states and operators as well as the concept of quantum hitting time, and we construct the quantum analogue of random walks. We discuss uses of quantum walks in search problems in Section 3.4.

Our novel contributions begin in Chapter 4, where we construct our new controlled quantum walk. We show that its stationary eigenvector is a superposition of the quantum analogues of the random walk's stationary distribution and the target distribution. Our main contribution is in Chapter 5, where we prove that controlled quantum walks provide a quadratic speed-up for sampling over random walks with stopping rules. We find this result by combining our analysis of random walks with stopping rules and our analysis of quantum walks, which is the first connection between the two in the literature. In Chapter 6, we introduce classical and quantum interpolated walks, and show that we can embed quantum interpolated walks into controlled quantum walks.

1.1 Sampling

Sampling is the task of randomly generating a mathematical object from a set (which in this thesis is the set of vertices of a graph) so that the probabilities of the samples collected correspond to a target probability distribution. Sampling is a fundamental component of tasks such as systems modelling and stochastic simulation [MRR⁺53, Has70].

When the target probability distribution is fully known and well-studied, sampling is easy and can take constant time. It becomes a more difficult task when the target probability distribution is more complicated or not directly given, such as when we only know the relative probabilities of different states.

1.1.1 Rejection Sampling

Rejection sampling is an example of a sampling algorithm. It solves the *resampling problem*, where we have access to a black box which generates samples of a given probability distribution encoded by the vector $\vec{\sigma}$, where $\sigma_i > 0$ for all i . Our goal is to efficiently generate samples from a different probability distribution, the target distribution $\vec{\tau}$.

The optimal algorithm, proposed by von Neumann [vN51], is to accept or reject samples from the black box with some probability based on the sample actually taken, and to continue sampling from the black box until we accept a sample. The vector of acceptance probabilities to sample $\vec{\tau}$ from $\vec{\sigma}$ is $\gamma \frac{\vec{\tau}}{\vec{\sigma}}$ with division taken entry-wise, where the optimal γ is the largest possible value that keeps probabilities to at most 1. This optimal value of γ is $\min \frac{\vec{\sigma}}{\vec{\tau}}$.

We can cast rejection sampling as a special case of sampling over vertices of a random walk. We show how our quantum algorithm provides a quadratic speed-up over rejection sampling in Section 5.1.1.

1.2 Random Walks

A *random walk* is a stochastic process on a graph, where we allow the graph to have directed or weighed edges [Lov93]. At each step of the process, a random walker is at one vertex of the graph. One step of the walk consists of the random walker moving to a randomly selected neighbouring vertex. The probability of walking to vertex j given that the random walker is at vertex i is proportional to the weight of the directed edge to j from i ,

denoted $w_{j\leftarrow i}$.

Formally, given a set of N vertices labelled from 1 to N , and given non-negative edge weights $w_{j\leftarrow i}$ for every pair of vertices j and i , a random walker at vertex i will walk to vertex j in the next step with probability

$$P_{j\leftarrow i} = \frac{w_{j\leftarrow i}}{\sum_k w_{k\leftarrow i}}. \quad (1.1)$$

The matrix P with elements $P_{j\leftarrow i}$ is the *transition matrix* for the random walk. We will refer to P as the random walk for convenience.

The location of the random walker at each step t is a random variable X_t . Because the probability of the walker being in a particular vertex $X_t = x_t$ depends only on the value of the variable X_{t-1} and the walk P , and not on other variables or t itself, the sequence X_0, X_1, \dots is *memoryless*, and is a time-homogenous Markov chain.

We can represent the probabilities of the walker being at each vertex by a probability distribution vector (a vector of non-negative real numbers which sum to 1). We use column vectors, as that matches their use for states in quantum computing. This differs from the more common usage in the random walk literature which is to use row vectors for probability distributions.

Given an initial probability distribution $\vec{\sigma}$, taking one step of the random walk results in the probability distribution $P\vec{\sigma}$ (note the left-multiplication from using column vectors). It follows that the probability distribution after t steps of the walk is $P^t\vec{\sigma}$.

1.2.1 Stationary Distribution

The sum of matrix elements of a given column i in P is

$$\begin{aligned} \sum_j P_{j\leftarrow i} &= \sum_j \frac{w_{j\leftarrow i}}{\sum_k w_{k\leftarrow i}} \\ &= \frac{\sum_j w_{j\leftarrow i}}{\sum_k w_{k\leftarrow i}} \\ &= 1. \end{aligned}$$

Matrices whose columns sum to 1 and whose entries are non-negative are *column-stochastic*, and map probability distribution vectors to probability distribution vectors. The row vector $(1, 1, \dots, 1)$ is then a left $(+1)$ -eigenvector of the matrix P . This implies that there is a right $(+1)$ -eigenvector for P . This vector is a *stationary distribution* of P .

1.2.2 Special Properties of Random Walks

There are three special properties that random walks can have. We assume that all three hold in our construction of their analogous quantum walks.

1. In *irreducible* walks, every vertex is reachable in a finite number of steps from every other vertex. Irreducible walks have a unique stationary distribution by the Perron-Frobenius theorem [Per07, Fro12]. The converse is not necessarily true: for instance, the random walk of two vertices where one step of the walk always brings the walker to vertex 2,

$$\begin{pmatrix} 0 & 0 \\ 1 & 1 \end{pmatrix},$$

has the unique stationary distribution

$$\begin{pmatrix} 0 \\ 1 \end{pmatrix}$$

and is reducible (i.e. reduces to two strongly connected components) since we cannot reach vertex 1 from vertex 2.

2. In *aperiodic* walks, there is no integer that divides the length of all directed cycles on the graph. A torus with even side lengths is an example of a *periodic* walk, since if we coloured it with a checkerboard pattern then the random walker would alternate colours with each step, making each cycle length a multiple of two.

An irreducible and aperiodic walk, called an *ergodic* walk, has a single eigenvalue with absolute value 1, which corresponds to the unique stationary distribution $\vec{\pi}$. This im-

plies that any probability distribution $\vec{\sigma}$ eventually converges to $\vec{\pi}$,

$$\lim_{t \rightarrow \infty} P^t \vec{\sigma} = \vec{\pi}.$$

3. In *reversible* walks, the walk is ergodic and the stationary distribution satisfies the detailed balance equation,

$$P_{j \leftarrow i} \pi_i = P_{i \leftarrow j} \pi_j. \quad (1.2)$$

The intuition for the term *reversible* is that running the random walk and playing it backwards are indistinguishable statistically. A useful property of reversible walks, which we use in connection to quantum walks, is that all of their eigenvalues are real.

1.2.3 Edge Weights of Reversible Walks

An ergodic walk whose edge weights are symmetric, i.e. $w_{j \leftarrow i} = w_{i \leftarrow j}$ for all j and i , has its stationary distribution equal to the sum of all outgoing (or equivalently incoming) edge weights for each vertex,

$$\pi_i = \frac{\sum_j w_{j \leftarrow i}}{\sum_{\ell, k} w_{\ell \leftarrow k}}. \quad (1.3)$$

We can normalize the edge weights by setting their sum $\sum_{\ell, k} w_{\ell \leftarrow k} = 1$, thus simplifying the above to $\pi_i = \sum_j w_{j \leftarrow i}$. We show that this is the correct stationary distribution of P by direct calculation, using the notation \vec{i} to refer to unit vectors,

$$\begin{aligned} P \sum_i \vec{i} \sum_j w_{j \leftarrow i} &= \sum_k \vec{k} \sum_i P_{k \leftarrow i} \sum_j w_{j \leftarrow i} \\ &= \sum_k \vec{k} \sum_i \frac{w_{k \leftarrow i}}{\sum_{\ell} w_{\ell \leftarrow i}} \sum_j w_{j \leftarrow i} \\ &= \sum_k \vec{k} \sum_i w_{k \leftarrow i} \\ &= \sum_k \vec{k} \sum_i w_{i \leftarrow k}. \end{aligned}$$

In addition, symmetric edge weights for an ergodic walk satisfy the detailed balance equation and so imply reversibility,

$$\begin{aligned}
P_{j \leftarrow i} \pi_i &= \frac{w_{j \leftarrow i}}{\sum_{\ell} w_{\ell \leftarrow i}} \sum_k w_{k \leftarrow i} \\
&= w_{j \leftarrow i} \\
&= w_{i \leftarrow j} \\
&= P_{i \leftarrow j} \pi_j.
\end{aligned}$$

The converse is also true: any reversible walk also corresponds to an ergodic walk with symmetric edge weights. We set the weights to be

$$w_{j \leftarrow i} = P_{j \leftarrow i} \pi_i, \tag{1.4}$$

where the symmetry $w_{j \leftarrow i} = w_{i \leftarrow j}$ follows directly from the detailed balance equation. This construction implies the identity $\pi_i = \sum_j w_{j \leftarrow i}$, which implies that the transition probabilities in Equation 1.1 remain consistent. Normalized edge weights of reversible walks are the probabilities that flow along each edge after taking one step from the stationary distribution.

1.2.4 Discriminant Matrix

Since P is not necessarily a normal matrix (a class of matrices which includes real symmetric matrices), its eigenvectors are not necessarily orthogonal. If P is reversible, however, following Szegedy [Sze04] there is an easily constructed similar matrix to P , called the *discriminant matrix* D . It is symmetric and hence has orthogonal eigenvectors, and we obtain it by

$$D = \sqrt{P \circ P^T}, \tag{1.5}$$

where the (Hadamard) product and square root of matrices are both entry-wise. Using the detailed balance equation, we may rewrite the matrix elements of D as

$$\begin{aligned} D_{j \leftarrow i} &= \sqrt{P_{j \leftarrow i} P_{i \leftarrow j}} \\ &= \sqrt{P_{j \leftarrow i}^2 \frac{\pi_i}{\pi_j}} \\ &= \frac{1}{\sqrt{\pi_j}} P_{j \leftarrow i} \sqrt{\pi_i} \end{aligned}$$

which gives a second form for D ,

$$D = \text{diag}(\sqrt{\pi})^{-1} P \text{diag}(\sqrt{\pi}). \quad (1.6)$$

The similarity transformation of Equation 1.6 shows that D is similar to P , and thus has the same eigenvalues. We can obtain eigenvectors of D by dividing eigenvectors of P entry-wise by $\sqrt{\pi}$. In particular, the unique $(+1)$ -eigenvector of D is $\sqrt{\pi}$.

1.3 Quantum Walks

Quantum walks are the quantum computing analogue of random walks, which we discuss in further detail in Section 3.3. They can solve certain problems asymptotically faster than the corresponding optimal classical algorithm.

One problem that quantum walks solve faster is the disjointness problem, where two parties have bit strings of length N and want to determine whether there is some position where both bit strings have value 1. Classically, a worst-case input requires $\Theta(N)$ bits of communication. There is a quantum walk algorithm that solves the disjointness problem using $\mathcal{O}(\sqrt{N})$ qubits [HdW02, AA03], a quadratic improvement.

Quantum walks can also solve the element distinctness problem, the problem of determining if there exist two elements in a set of N which are identical. Classically, this requires $\Omega(N)$ queries in the worst case, whereas a quantum walk algorithm can solve it in $\Theta(N^{2/3})$ queries [Amb04].

Quantum walks can also solve the problems of detecting and finding marked vertices on a graph, which we describe in more detail in Section 3.4.

Chapter 2

Sampling Using Random Walks with Stopping Rules

A random walk by itself does not have a stopping condition, and so does not directly produce probability distributions. We can sample from a probability distribution by adding a *stopping rule* to the walk. The presentation of stopping rules throughout this chapter follows that of Lovász and Winkler [LW95].

A stopping rule for a random walk is a set of conditions that determine when the walk should stop. Once a walk has stopped after starting in some probability distribution $\vec{\sigma}$, the vertex in which it stopped is a sample from some new probability distribution, which by construction is the target distribution $\vec{\tau}$.

The conditions for stopping can include the number of steps taken, the current vertex of the random walker, and a probabilistic choice. In general, a stopping rule is a function from the set of possible paths on the underlying graph to a probability of stopping.

2.1 Access Time

The expected number of steps that a random walk P takes before stopping, given that we began in an initial probability distribution $\vec{\sigma}$, is the *access time* of the stopping rule. For a given walk, initial distribution, and target distribution, we denote the access time of an optimal stopping rule from the initial to the target distribution as $HT(P, \vec{\sigma} \rightarrow \vec{\tau})$.

We use the notation HT because access times relate to the concept of *hitting times*. The hitting time is the expected number of steps before stopping in one of a subset of vertices, called marked vertices. The two are equal if we set $\vec{\tau}$ to be the resultant distribution of a stopping rule which is to stop exactly when we reach a marked vertex.

2.2 Exit Frequencies

For each vertex i of the graph, the expected number of times that the walk will exit that vertex (and so enter a new one) before stopping is the *exit frequency* for that vertex. The vector \vec{x} of exit frequencies satisfies $\|\vec{x}\|_1 = \text{HT}(\mathbb{P}, \vec{\sigma} \rightarrow \vec{\tau})$, since the expected number of steps before stopping is exactly the expected total number of times the walk will exit vertices.

The exit frequencies are the key ingredient to the connection between random walks with stopping rules and the quantum walks we introduce in Section 4.1. Exit frequencies are a kind of encoding for entire history of the walk as well as the relationship between the initial and target distributions, via the identity

$$\mathbb{P}\vec{x} = \vec{x} + \vec{\tau} - \vec{\sigma}. \quad (2.1)$$

Expressed in the form $\vec{\tau} = \mathbb{P}\vec{x} + \vec{\sigma} - \vec{x}$, the identity states that in order to stop at a vertex (according to $\vec{\tau}$), we must have reached this vertex after having exited another ($\mathbb{P}\vec{x}$) or have started in it directly ($\vec{\sigma}$), without having then exited it ($-\vec{x}$).

If two stopping rules for the same random walk have the same initial and final distributions, then both their exit frequency vectors \vec{x}_1 and \vec{x}_2 satisfy Equation 2.1. In particular,

$$\mathbb{P}(\vec{x}_1 - \vec{x}_2) = \vec{x}_1 - \vec{x}_2$$

so \vec{x}_1 and \vec{x}_2 differ by a multiple of a stationary distribution of \mathbb{P} . If \mathbb{P} is irreducible, then they differ by a multiple of the unique stationary distribution $\vec{\pi}$. Conversely, by rewriting Equation 2.1 as $(\mathbb{P} - \mathbb{1})\vec{x} = \vec{\tau} - \vec{\sigma}$ we can see that if two stopping rules differ by a stationary distribution of \mathbb{P} , then their target distribution is the same for the same initial distribution.

We can obtain the exit frequencies of an optimal stopping rule by finding the solution to Equation 2.1 which minimizes $\|\vec{x}\|_1$. For irreducible walks, we find any solution to Equation 2.1 and subtract a multiple of $\vec{\pi}$ such that the smallest element of \vec{x} is 0 (i.e., at

least one vertex is absorbing, meaning that the walk always stops if it reaches the absorbing vertex).

2.3 Local Stopping Rules

A local stopping rule is a stopping rule that depends only on the current vertex of the walker at each given step. That is, the stopping rule function depends only on the last vertex in the random walker's path, so we can specify it by a vector of stopping probabilities \vec{q} . Local stopping rules are memoryless like the random walk itself, and so require minimal overhead to implement.

We can construct a local stopping rule from the optimal exit frequencies \vec{x} as follows. For each vertex i , the expected number of times we exit the state and keep walking is x_i , and the expected number of times we stop in that vertex (which is the probability that we stop in that vertex) is τ_i . Thus, the overall probability that we stop in vertex i upon reaching it is

$$q_i = \frac{\tau_i}{x_i + \tau_i}. \quad (2.2)$$

Equation 2.2 is thus a necessary condition for the local stopping rule.

We argue that these local stopping probabilities are sufficient to generate $\vec{\tau}$ from $\vec{\pi}$ by an argument from contradiction. If the local stopping rule produced a final distribution $\vec{\tau}'$ distinct from $\vec{\tau}$, then there would be some vertices where $\tau'_i > \tau_i$ and other vertices where $\tau'_i < \tau_i$. Because the local stopping rule ensures that $\vec{\tau}' / \vec{x}' = \vec{\tau} / \vec{x}$, the vertices with higher stopping probabilities will also have higher exit frequencies than the exit frequencies for the target distribution $\vec{\tau}$. This implies that the local stopping rule results in a walk that enters those vertices where $\tau'_i > \tau_i$ more often than a stopping rule that stops in $\vec{\tau}$.

The local stopping probabilities thus cannot generate a distribution distinct from $\vec{\tau}$. The underlying graph P has not changed, and the only difference between the local stopping rule and a rule that generates $\vec{\tau}$ is when we stop, not how we move before stopping.

There is no mechanism by which a random walk modified only by stopping rules can enter one class of vertices more often while exiting the other class of vertices less often.

Chapter 3

Quantum Walks

3.1 Quantum States and Operators

In quantum computing, we represent the state of a system as a *ket*, which is a column vector in a Hilbert space. For example, a classical bit which can take on the values 0 and 1 becomes a qubit in the Hilbert space \mathcal{H}_2 , whose computational basis states are $|0\rangle$ and $|1\rangle$. The conjugate transpose of a ket, which is a row vector, is a *bra* (hence the term “bra(c)ket notation”) and we represent it as $\langle\psi|$.

For any set of quantum states in the same space, any normalized linear combination, or superposition, of them is also a valid quantum state. Thus, the state $\frac{1}{\sqrt{2}}(|0\rangle + |1\rangle) = |+\rangle$ is a valid qubit state.

The probability to measure a basis state $|\phi\rangle$ when we have the state $|\psi\rangle$ is $|\langle\phi|\psi\rangle|^2$. Because the probabilities over all orthonormal basis states must sum to one, quantum states have a 2-norm of one, i.e. they are 2-normalized.

Because physical quantum states are always normalized, the allowed operations on quantum states must preserve norms. This class of operators is the unitary operators. The eigenvalues of a unitary operator are on the unit circle, so we can write them as $e^{i\theta}$ for some real *eigenphase* $\theta \in (-\pi, \pi]$. Another property of unitary operators is that the adjoint \dagger of the operator (or conjugate transpose of the matrix) is the inverse of the operator, which in particular implies that all quantum operators are invertible.

In this thesis, all operators we consider are also real-valued unitary operators in some basis (i.e. they are orthogonal matrices when written in that basis). This implies, by the complex conjugate root theorem, that the eigenvalues come in complex conjugate pairs $e^{\pm i\theta}$, with the corresponding eigenstates being complex conjugates of each other.

For more general introductions to quantum computing, see [Mer07, dW16].

3.2 Quantum Hitting Time

Our quantum algorithm, which we introduce in Chapter 4, works within the framework of the quantum phase estimation algorithm [CEMM98]. Phase estimation is a quantum algorithm which approximately isolates the $(+1)$ -eigenvector of an operator, when the input is a state that overlaps it.

Theorem 1 (Phase Estimation) [CEMM98, DH17] *Given any unitary operator W with spectrum*

$$W = |\lambda_0\rangle\langle\lambda_0| + \sum_i e^{i\theta_i} |\lambda_i\rangle\langle\lambda_i|$$

and a starting state $|\psi\rangle$, we can isolate a state with constant overlap with the unique $(+1)$ -eigenvector $|\lambda_0\rangle$ using

$$\Theta\left(\frac{\text{QHT}(W, |\psi\rangle)}{|\langle\lambda_0|\psi\rangle|}\right)$$

applications of W and with success probability $|\langle\lambda_0|\psi\rangle|^2$, where

$$\text{QHT}(W, |\psi\rangle) = \sqrt{\sum_i |\langle\lambda_i|\psi\rangle|^2 \cot\left(\frac{\theta_i}{2}\right)}. \quad (3.1)$$

The strategy we use is to construct an operator whose unique $(+1)$ -eigenvector is an equal superposition of the initial state and the target state. Our algorithm does not require direct knowledge of the target state, as we only need to know the target probabilities relative to the initial probabilities as we explain further in Section 4.1.

By running phase estimation, we can isolate the $(+1)$ -eigenvector with $1/2$ probability, and find a different eigenstate with $1/2$ probability. If we have the $(+1)$ -eigenvector, we perform a second measurement of an ancilla qubit, which with $1/2$ probability is $|1\rangle$ and collapses the state to the target state, and with $1/2$ probability is $|0\rangle$ and collapses

it back to the initial state. The overall algorithm thus has a success probability of $1/4$ to generate the target state from the initial state.

In our calculations, we find the quantum hitting time not by using Equation 3.1, which involves a full spectral analysis of the operator, but by using another formula in Lemma 2, which involves finding the $(+1)$ -eigenvector of a related operator.

Lemma 2 *Given a real unitary W whose unique $(+1)$ -eigenvector is $|\lambda_0\rangle$ and given a starting state $|\psi\rangle$, there is a unique $(+1)$ -eigenvector of the operator $W(\mathbb{1} - 2|\lambda_0\rangle\langle\lambda_0|)(\mathbb{1} - 2|\psi\rangle\langle\psi|)$, which we denote as $|\kappa\rangle$. We can calculate the quantum hitting time from $|\kappa\rangle$ as follows [DH17],*

$$\text{QHT}^2(W, |\psi\rangle) = \frac{1}{|\langle\kappa|\psi\rangle|^2} - 1. \quad (3.2)$$

3.3 Construction of Quantum Walks

We can construct a *quantum walk* following the construction by Szegedy [Sze04] and Ambainis, Kempe, and Rivosh [AKR05]. The walk is on the *edges* of the graph, instead of on the vertices as in random walks; this ensures that the resulting operator is unitary and therefore invertible. For each vertex i , we use the state $|i\rangle$ to represent the vertex, and for each edge from vertex i to vertex j , we use the state $|i, j\rangle$ to represent the edge. This is a shorthand for the tensor product state $|i\rangle \otimes |j\rangle = |i\rangle|j\rangle = |i, j\rangle$, and it represents having one quantum register in the vertex state $|i\rangle$ and another in the state $|j\rangle$.

We define the canonical superposition of the neighbours of vertex i in a reversible walk P as

$$|p_i\rangle = \sum_j \sqrt{P_{j \leftarrow i}} |j\rangle \quad (3.3)$$

and we construct the following isometry which maps from the vertex space to the edge space,

$$T = \sum_i |i, p_i\rangle\langle i| = \sum_{i,j} \sqrt{P_{j \leftarrow i}} |i, j\rangle\langle i|. \quad (3.4)$$

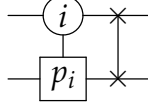


Figure 3.1: The quantum walk as the set of reflections about $|i, p_i\rangle$ followed by SWAP

The other important operator we use is the self-inverse operator SWAP which reverses the direction of edges,

$$S = \sum_{i,j} |j, i\rangle\langle i, j|. \quad (3.5)$$

We define the quantum walk operator as a reflection about the neighbours of each vertex followed by a swap of all edges,

$$W = S(2TT^\dagger - \mathbb{1}) = S\left(2\sum_i |i, p_i\rangle\langle i, p_i| - \mathbb{1}\right), \quad (3.6)$$

which we represent as a quantum circuit in Figure 3.1. Note that because we represent quantum states as column vectors, composed operations apply to states from right to left when written algebraically.

The stationary eigenvector of a walk under Szegedy's construction is the quantum analogue $T\sqrt{\vec{\pi}}$ of the stationary distribution $\vec{\pi}$, which we denote as

$$|\text{init}\rangle = \sum_i \sqrt{\pi_i} |i, p_i\rangle = \sum_{i,j} \sqrt{P_{j\leftarrow i}} \sqrt{\pi_i} |i, j\rangle \quad (3.7)$$

and it satisfies $(2\sum_i |i, p_i\rangle\langle i, p_i| - \mathbb{1})|\text{init}\rangle = |\text{init}\rangle$ by construction.

Using normalized edge weights as defined in Equation 1.4, we can also see that

$$|\text{init}\rangle = \sum_{i,j} \sqrt{w_{j\leftarrow i}} |i, j\rangle$$

and since the underlying walk P is reversible, this implies that $S|\text{init}\rangle = |\text{init}\rangle$, and hence $W|\text{init}\rangle = |\text{init}\rangle$.

3.3.1 Szegedy's Correspondence

Consider the operator $T^\dagger S T$ which acts on the vertex space. A state $|i\rangle$ corresponding to vertex i under this operator maps to

$$\begin{aligned}
 T^\dagger S T |i\rangle &= T^\dagger S |i, p_i\rangle \\
 &= T^\dagger |p_i, i\rangle \\
 &= \sum_j |j\rangle \langle j | p_i \rangle \langle p_j | i \rangle \\
 &= \sum_j \sqrt{P_{j \leftarrow i} P_{i \leftarrow j}} |j\rangle \\
 &= D |i\rangle.
 \end{aligned}$$

Since this is true for all vertex states $|i\rangle$, it follows that

$$T^\dagger S T = D. \tag{3.8}$$

Now consider an eigenvector $|\lambda\rangle$ of D with eigenvalue $\lambda \neq 1$. Since D has the same eigenvalues as P , and since we assume that P is reversible, $-1 < \lambda < 1$, so we may write $\lambda = \cos(\theta)$. If we apply the walk $W = S(2TT^\dagger - \mathbb{1})$ to the edge space vector $T|\lambda\rangle$, we obtain

$$\begin{aligned}
 S(2TT^\dagger - \mathbb{1})T|\lambda\rangle &= 2STT^\dagger T|\lambda\rangle - ST|\lambda\rangle \\
 &= 2ST|\lambda\rangle - ST|\lambda\rangle \\
 &= ST|\lambda\rangle
 \end{aligned}$$

where we use that $T^\dagger T = \mathbb{1}$ because T is an isometry.

If we apply the quantum walk to this state $ST|\lambda\rangle$, we obtain

$$\begin{aligned}
 S(2TT^\dagger - \mathbb{1})ST|\lambda\rangle &= 2STT^\dagger ST|\lambda\rangle - SST|\lambda\rangle \\
 &= 2STD|\lambda\rangle - T|\lambda\rangle \\
 &= 2\cos(\theta)ST|\lambda\rangle - T|\lambda\rangle.
 \end{aligned}$$

We thus see that the subspace spanned by $T|\lambda\rangle$ and $ST|\lambda\rangle$ is invariant under the action of W . As this is a two-dimensional space spanned by real vectors and W is a real unitary, this subspace is a two-dimensional rotational space. The angle of rotation is

$$\begin{aligned}\cos^{-1}((ST|\lambda\rangle)^\dagger(T|\lambda\rangle)) &= \cos^{-1}(\langle\lambda|T^\dagger ST|\lambda\rangle) \\ &= \cos^{-1}(\langle\lambda|D|\lambda\rangle) \\ &= \theta.\end{aligned}$$

Since $|\lambda\rangle$ relates to the corresponding eigenvector $\vec{\lambda}$ of P by

$$|\lambda\rangle = \frac{\vec{\lambda}}{\sqrt{\vec{\pi}}},$$

where the division is entry-wise, it follows that each eigenvector of P with eigenvalue $\cos(\theta)$ corresponds to a rotational space in two dimensions of W with rotational angle θ .

Note that repeated applications of W to states of the form $T\vec{w}$ will always stay in the span of states of the form $T\vec{w}$ and $ST\vec{w}$, or equivalently the span of states of the form $|i, p_i\rangle$ and $|p_i, i\rangle$. This relevant space is of dimension $2N - 1$, because there is one dimension corresponding to the $(+1)$ -eigenvector $|\text{init}\rangle$, and $N - 1$ two-dimensional rotational spaces. We refer to this space as \mathcal{H}_W . By construction, $|\text{init}\rangle$ is the unique $(+1)$ -eigenvector of W in \mathcal{H}_W .

We can also derive the mathematical objects and relations used in this thesis from any real unitary operator with a unique $(+1)$ -eigenvector, which we describe in detail in Appendix B.

3.4 Detecting and Finding

Two main types of problems that quantum walks can solve quadratically faster than classically are the *detecting* and *finding* problems on graphs. Both involve splitting the graph into marked and unmarked vertices as detailed further in Section 5.2. The detecting problem is the problem of determining whether marked vertices exist in the graph, and the

finding problem is the problem of identifying any particular marked vertex if at least one exists.

Both finding and detecting on the complete graph are solvable using Grover's search algorithm [Gro96], which is quadratically faster than a random walk on the complete graph (the equivalent of sampling vertices randomly until we find a marked vertex). More generally, we can convert any quantum algorithm with a success probability of p to find a marked state into another quantum algorithm with constant success probability using $1/\sqrt{p}$ applications of both the original algorithm and of a reflection of the marked states, using the amplitude amplification algorithm [BHMT02].

Applying amplitude amplification directly to random walks has the disadvantage of repeatedly reflecting the $(+1)$ -eigenvector $|\text{init}\rangle$, a superposition of all edges, whereas quantum walks only use a single copy of $|\text{init}\rangle$ at the beginning of their application then use operations that only affect neighbours in any individual step. Interleaving the quantum walk step W with a reflection of the marked states, and embedding this in phase estimation, solves the detection problem quadratically faster than quantum walks, and solves the finding problem if there is a unique marked vertex [Sze04, AKR05]. Interpolated walks [KMOR16], which we discuss as they apply to sampling in Chapter 6, as well as quantum fast-forwarding [AS19], can both solve the finding problem quadratically faster than random walks [AGJK20].

Quantum interpolated walks [KMOR16] and controlled quantum walks [DH17] can sample from the stationary distribution limited to marked vertices (which solves the finding problem), and do so quadratically faster than the *extended hitting time*, which as we show in Section 6.4 is upper-bounded by the access time for the analogous classical sampling. We generalize these models in Section 4.1 so that we can sample from any distribution of vertices.

Chapter 4

Controlled Quantum Walks

Our novel contribution begins in this chapter, where we construct a controlled quantum walk which can sample from probability distributions quadratically faster than random walks. We then prove the speed-up in Chapter 5. We generalize the controlled quantum walk circuit from Dohotaru and Høyer [DH17] to have a different control angle for each vertex. This allows us to sample from the quantum analogue of the target distribution $\vec{\tau}$,

$$|\tau\rangle = \sum_i \sqrt{\tau_i} |i, p_i\rangle. \quad (4.1)$$

We also use scaled versions of $\vec{\tau}$ and $|\tau\rangle$ using the scaling parameter p_τ (which in practice is close or equal to 1) as

$$\begin{aligned} \vec{\tau}_{\text{un}} &= p_\tau \vec{\tau} \\ |\tau_{\text{un}}\rangle &= \sqrt{p_\tau} |\tau\rangle. \end{aligned}$$

4.1 Construction

We first define the vector of control angles entry-wise as

$$\cos^2(\theta_i) = \frac{\tau_{\text{un},i}}{\pi_i + \tau_{\text{un},i}} = \left(\frac{\pi_i}{\tau_{\text{un},i}} + 1 \right)^{-1} \quad (4.2)$$

with $\theta_i \in (0, \pi/2]$. We exclude $\theta_i = 0$ because $\pi_i \neq 0$ for all i in irreducible walks, and so $\cos^2(\theta_i) < 1$. We have the angle $\theta_i = \pi/2$ when $\tau_{\text{un},i} = 0$. Note that we can compute the angles solely from the individual ratios between π_i and $\tau_{\text{un},i}$. This means that an implementation can calculate all of the angles in superposition.

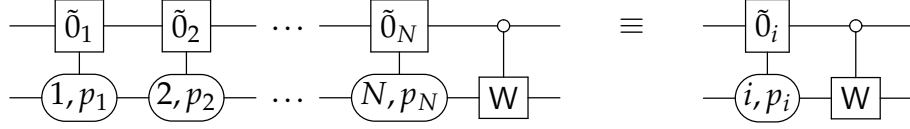


Figure 4.1: The circuit $U(\vec{\theta})$

We also define the rotated qubit bases $\{|\tilde{0}_i\rangle, |\tilde{1}_i\rangle\}$ for each i as

$$\begin{aligned}
|\tilde{0}_i\rangle &= \cos(\theta_i)|0\rangle + \sin(\theta_i)|1\rangle = \sqrt{\frac{\tau_{\text{un},i}}{\pi_i + \tau_{\text{un},i}}}|0\rangle + \sqrt{\frac{\pi_i}{\pi_i + \tau_{\text{un},i}}}|1\rangle \\
|\tilde{1}_i\rangle &= -\sin(\theta_i)|0\rangle + \cos(\theta_i)|1\rangle = -\sqrt{\frac{\pi_i}{\pi_i + \tau_{\text{un},i}}}|0\rangle + \sqrt{\frac{\tau_{\text{un},i}}{\pi_i + \tau_{\text{un},i}}}|1\rangle
\end{aligned} \tag{4.3}$$

where we note that $\langle 1|\tilde{0}_i\rangle \neq 0$ for all i .

The controlled quantum walk $U(\vec{\theta})$ consists of N reflections of $|\tilde{0}_i\rangle$ controlled by each $|i, p_i\rangle$, followed by W controlled by $|0\rangle$, as shown in the left-hand side of Figure 4.1. A physical implementation can perform the N initial reflections as a single controlled operation, by having a quantum subroutine that calculates the angle of reflection based on the state of the walk register, as shown in the right-hand side of the figure.

Note that states of the form $|i, p_i\rangle$ in the walk register control the first N reflections. These are the only operations in $U(\vec{\theta})$ that affect a state of $|1\rangle$ in the ancilla non-trivially, since $|0\rangle$ controls W . If we start in states of the form $|0\rangle \otimes T\vec{w}$, then whenever we have $|1\rangle$ in the ancilla we will always have a superposition of states of the form $|i, p_i\rangle$ in the walk register.

The relevant space for $U(\vec{\theta})$ is thus the span of $|0\rangle \otimes \mathcal{H}_W$ and the N states of the form $|1\rangle|i, p_i\rangle$. We refer to this space of dimension $3N - 1$ as \mathcal{H}_U (note that the space does not depend on $\vec{\theta}$).

4.2 Stationary Eigenvector

Lemma 3 *The unique (up to scalars) $(+1)$ -eigenvector of $U(\vec{\theta})$ in \mathcal{H}_U is*

$$|U_0\rangle = \frac{1}{\sqrt{1 + p_\tau}}(|0, \text{init}\rangle - \sqrt{p_\tau}|1, \tau\rangle) = \frac{1}{\sqrt{1 + p_\tau}}(|0, \text{init}\rangle - |1, \tau_{\text{un}}\rangle). \tag{4.4}$$

Proof We rewrite a scaled version of $|U_0\rangle$ as

$$\begin{aligned}
\sqrt{1+p_\tau}|U_0\rangle &= \sum_i (\sqrt{\pi_i}|0\rangle - \sqrt{\tau_{\text{un},i}}|1\rangle)|i,p_i\rangle \\
&= \sum_i \sqrt{\pi_i} \left(|0\rangle - \sqrt{\frac{\tau_{\text{un},i}}{\pi_i}}|1\rangle \right) |i,p_i\rangle \\
&= \sum_i \frac{\sqrt{\pi_i}}{\sin(\theta_i)} (\sin(\theta_i)|0\rangle - \cos(\theta_i)|1\rangle) |i,p_i\rangle \\
&= - \sum_i \frac{\sqrt{\pi_i}}{\sin(\theta_i)} |\tilde{1}_i\rangle |i,p_i\rangle.
\end{aligned}$$

Because $|\tilde{1}_i\rangle$ is orthogonal to $|\tilde{0}_i\rangle$ for each i , it follows that the first N reflections of $U(\vec{\theta})$ have no effect on the $(+1)$ -eigenvector. From Equation 4.4, applying W conditioned on $|0\rangle$ will also have no effect because $|\text{init}\rangle$ is a $(+1)$ -eigenvector of W .

We can prove that $|U_0\rangle$ is the unique $(+1)$ -eigenvector of $U(\vec{\theta})$ in \mathcal{H}_U by using the *flip-flop lemma*, which we prove in Appendix A and state below.

Lemma 4 (Flip-flop lemma) [Doh15] *Let A be a real unitary operator, and let $|\psi\rangle$ be a real state. Let d_+ be the dimensionality of the $(+1)$ -eigenspace of A . The dimensionality of the operator $A(\mathbb{1} - 2|\psi\rangle\langle\psi|)$ is $(d_+ - 1)$ if $|\psi\rangle$ overlaps the $(+1)$ -eigenspace of A , and it is $(d_+ + 1)$ if $|\psi\rangle$ does not overlap the $(+1)$ -eigenspace of A .*

Because W has a unique $(+1)$ -eigenvector $|\text{init}\rangle$ in \mathcal{H}_W , and \mathcal{H}_U consists of the direct sum of $|0\rangle \otimes \mathcal{H}_W$ and the N -dimensional subspace spanned by states of the form $|1\rangle|i,p_i\rangle$, it follows that W controlled by $|0\rangle$ has $(1 + N)$ $(+1)$ -eigenvectors in \mathcal{H}_U . Each reflection of $|\tilde{0}_i\rangle|i,p_i\rangle$ in $U(\vec{\theta})$ overlaps $|1\rangle|i,p_i\rangle$, so after N applications of the flip-flop lemma, the remaining $(+1)$ -eigenspace of the full operator $U(\vec{\theta})$ has dimension exactly 1, making $|U_0\rangle$ the unique $(+1)$ -eigenvector of $U(\vec{\theta})$ in \mathcal{H}_U . \square

Chapter 5

Quadratic Speed-Up Over Access Time

In this chapter, we prove our main result that our controlled quantum walk samples from probability distributions quadratically faster than random walks with stopping rules. We do this by showing how to use $U(\vec{\theta})$ within phase estimation to generate the quantum state $|\tau\rangle$ which is analogous to the target distribution $\vec{\tau}$. We can begin the controlled quantum walk with the state $|\text{init}\rangle$, which is the analogous state to $\vec{\pi}$, or $|\overline{\text{init}}\rangle$, which is $|\text{init}\rangle$ limited to a set of unmarked vertices.

We prove that the quantum hitting time of our new controlled quantum walk is of order the square root of the access time from $\vec{\pi}$ to $\vec{\tau}$, i.e.

$$\text{QHT}(U(\vec{\theta}), |0, \text{init}\rangle) \in \Theta\left(\sqrt{\text{HT}(\mathcal{P}, \vec{\pi} \rightarrow \vec{\tau})}\right), \quad (5.1)$$

and we have a similar quadratic speed-up when starting in $|\overline{\text{init}}\rangle$,

$$\text{QHT}(U(\vec{\theta}), |0, \overline{\text{init}}\rangle) \in \Theta\left(\sqrt{\text{HT}(\mathcal{P}, \vec{\pi} \rightarrow \vec{\tau})}\right), \quad (5.2)$$

where

$$\vec{\tau} = \frac{1}{\varepsilon + p_\tau} (p_\tau \vec{\tau} + \vec{\pi}_{\mathcal{M}}) \quad (5.3)$$

and $\vec{\pi}_{\mathcal{M}}$ is the stationary distribution limited to the set of marked vertices.

5.1 Starting in $|\text{init}\rangle$

The form of the $(+1)$ -eigenvector in Equation 4.4 suggests that we can produce the target state $|\tau\rangle$ from the stationary state $|\text{init}\rangle$ using phase estimation. For the purposes of calculating the quantum hitting time, we write the initial state with the ancilla qubit $|0, \text{init}\rangle$ as

a superposition of the $(+1)$ -eigenvector and an orthogonal vector. The orthogonal vector is

$$|\overline{0, \text{init}}\rangle = \frac{1}{\sqrt{1+p_\tau}}(\sqrt{p_\tau}|0, \text{init}\rangle + |1, \tau\rangle) \quad (5.4)$$

so that we can write

$$|0, \text{init}\rangle = \frac{1}{\sqrt{1+p_\tau}}|U_0\rangle + \sqrt{\frac{p_\tau}{1+p_\tau}}|\overline{0, \text{init}}\rangle. \quad (5.5)$$

The exact squared quantum hitting time of $U(\vec{\theta})$ starting in $|0, \text{init}\rangle$ is

$$\begin{aligned} \text{QHT}^2(U(\vec{\theta}), |0, \text{init}\rangle) &= \text{QHT}^2\left(U(\vec{\theta}), \frac{1}{\sqrt{1+p_\tau}}|U_0\rangle + \sqrt{\frac{p_\tau}{1+p_\tau}}|\overline{0, \text{init}}\rangle\right) \\ &= \frac{p_\tau}{1+p_\tau} \text{QHT}^2\left(U(\vec{\theta}), |\overline{0, \text{init}}\rangle\right). \end{aligned} \quad (5.6)$$

We use Lemma 2 to determine an exact form of the squared quantum hitting time using the vector $|\kappa\rangle$,

$$\begin{aligned} \text{QHT}^2(U(\vec{\theta}), |0, \text{init}\rangle) &= \frac{p_\tau}{1+p_\tau} \left(\frac{1}{|\langle \kappa | \overline{0, \text{init}} \rangle|^2} - 1 \right) \\ &= \frac{p_\tau}{1+p_\tau} \left(\frac{\|\kappa_{\text{un}}\|^2}{|\langle \kappa_{\text{un}} | \overline{0, \text{init}} \rangle|^2} - 1 \right). \end{aligned} \quad (5.7)$$

The form of the vector $|\kappa\rangle$ involves a quantum analogue of the exit frequencies \vec{x} . We define this quantum analogue $|x\rangle$ as

$$|x\rangle = (\mathbb{1} - S)\mathbb{T} \frac{\vec{x}}{\sqrt{\vec{\pi}}}. \quad (5.8)$$

Note that any state multiplied by $\mathbb{1} - S$, including $|x\rangle$, is a (-1) -eigenvector of S . This follows from $S(\mathbb{1} - S) = S - \mathbb{1}$. More generally, states of the form $|i, j\rangle - |j, i\rangle$ are (-1) -eigenvectors of S , and states of the form $|i, j\rangle + |j, i\rangle$ are $(+1)$ -eigenvectors of S .

Lemma 5 *The unique $(+1)$ -eigenvector of the operator*

$$U(\vec{\theta})(\mathbb{1} - 2|\overline{0, \text{init}}\rangle\langle\overline{0, \text{init}}|)(\mathbb{1} - 2|U_0\rangle\langle U_0|)$$

in \mathcal{H}_U is

$$|\kappa_x\rangle = |0, x\rangle + |0, \text{init}\rangle + \frac{1}{\sqrt{p_\tau}}|1, \tau\rangle = |0, x\rangle + \sqrt{\frac{1+p_\tau}{p_\tau}}|\overline{0, \text{init}}\rangle. \quad (5.9)$$

Proof We show that this is a $(+1)$ -eigenvector of $U(\vec{\theta})$ by direct calculation.

First, we show that $\langle U_0 | \kappa_x \rangle = 0$, making the state invariant under the first reflection. We can see this from the last formulation of $|\kappa_x\rangle$ in Equation 5.9, and from $|U_0\rangle$ being a superposition of $|0, \text{init}\rangle$ and $|1, \tau\rangle$. The first term $|0, x\rangle$ is orthogonal to $|0, \text{init}\rangle$ because $|x\rangle$ is a (-1) -eigenvector of S while $|\text{init}\rangle$ is a $(+1)$ -eigenvector of S , and $|0, x\rangle$ is also orthogonal to $|1, \tau\rangle$ because the ancilla qubits are orthogonal. The second term $|\overline{0, \text{init}}\rangle$ is orthogonal to $|U_0\rangle$ by construction in Section 4.2. We thus have that

$$(\mathbb{1} - 2|U_0\rangle\langle U_0|)|\kappa_x\rangle = |\kappa_x\rangle.$$

Second, we find the effect of the reflection of $|\overline{0, \text{init}}\rangle$. Because it too is a superposition of $|0, \text{init}\rangle$ and $|1, \tau\rangle$, it is orthogonal to $|0, x\rangle$. We thus negate the $|\overline{0, \text{init}}\rangle$ term to obtain

$$(\mathbb{1} - 2|\overline{0, \text{init}}\rangle\langle \overline{0, \text{init}}|)|\kappa_x\rangle = |0, x\rangle - \sqrt{\frac{1 + p_\tau}{p_\tau}}|\overline{0, \text{init}}\rangle. \quad (5.10)$$

Finally, we apply $U(\vec{\theta})$. We begin with its first step, the reflections of the N states $|\tilde{0}_i\rangle|i, p_i\rangle$. We use a specific superposition of these states,

$$\begin{aligned} \sum_i \sqrt{\frac{\tau_i}{p_\tau}} \frac{1}{\sin(\theta_i)} |\tilde{0}_i\rangle|i, p_i\rangle &= \sum_i \sqrt{\frac{\tau_i}{p_\tau}} (\cot(\theta_i)|0\rangle + |1\rangle)|i, p_i\rangle \\ &= \sum_i \sqrt{\frac{\tau_i}{p_\tau}} \left(\sqrt{\frac{\tau_{\text{un},i}}{\pi_i}}|0\rangle + |1\rangle \right) |i, p_i\rangle \\ &= \sum_i \left(\frac{\tau_i}{\sqrt{\pi_i}}|0\rangle + \sqrt{\frac{\tau_i}{p_\tau}}|1\rangle \right) |i, p_i\rangle \\ &= |0, \rho\rangle + \frac{1}{\sqrt{p_\tau}}|1, \tau\rangle \end{aligned}$$

where we have introduced the unnormalized state

$$|\rho\rangle = \sum_i \frac{\tau_i}{\sqrt{\pi_i}} |i, p_i\rangle = T \frac{\vec{\tau}}{\sqrt{\vec{\pi}}}. \quad (5.11)$$

We rewrite the intermediate state from Equation 5.10 as

$$|0, x\rangle - |0, \text{init}\rangle - \frac{1}{\sqrt{p_\tau}}|1, \tau\rangle = (|0, x\rangle - |0, \text{init}\rangle + |0, \rho\rangle) - \left(|0, \rho\rangle + \frac{1}{\sqrt{p_\tau}}|1, \tau\rangle \right).$$

The subtracted term gets reflected as it is a linear combination of the states $|\tilde{0}_i\rangle|i, p_i\rangle$, and the first term stays the same since $|\text{init}\rangle$ and $|\rho\rangle$ are in the image of T and

$$\begin{aligned}
T^\dagger|x\rangle &= T^\dagger(\mathbb{1} - S)T\frac{\vec{x}}{\sqrt{\vec{\pi}}} \\
&= (\mathbb{1} - D)\frac{\vec{x}}{\sqrt{\vec{\pi}}} \\
&= \frac{(\mathbb{1} - P)\vec{x}}{\sqrt{\vec{\pi}}} \\
&= \frac{\vec{x} - (\vec{x} + \vec{\tau} - \vec{\pi})}{\sqrt{\vec{\pi}}} \\
&= \frac{\vec{\pi} - \vec{\tau}}{\sqrt{\vec{\pi}}} \tag{5.12}
\end{aligned}$$

$$= T^\dagger(|\text{init}\rangle - |\rho\rangle). \tag{5.13}$$

The identity $T^\dagger|x\rangle = \frac{\vec{\pi} - \vec{\tau}}{\sqrt{\vec{\pi}}}$ in particular gives an intuition for why $|x\rangle$ is important to this proof: it encodes the relationship between the initial and the final state, in an analogous way to the classical identity $(\mathbb{1} - P) = \vec{\pi} - \vec{\tau}$ when starting in $\vec{\pi}$.

After the reflections, we thus have the state

$$\begin{aligned}
&(|0, x\rangle - |0, \text{init}\rangle + |0, \rho\rangle) + \left(|0, \rho\rangle + \frac{1}{\sqrt{p_\tau}}|1, \tau\rangle\right) \\
&= |0, x\rangle - |0, \text{init}\rangle + 2|0, \rho\rangle + \frac{1}{\sqrt{p_\tau}}|1, \tau\rangle.
\end{aligned}$$

The final operation is W controlled by $|0\rangle$, so we consider only the part of the state with $|0\rangle$ in the ancilla qubit,

$$\begin{aligned}
W(|x\rangle - |\text{init}\rangle + 2|\rho\rangle) &= S(2TT^\dagger - \mathbb{1})(|\rho\rangle + (|x\rangle - |\text{init}\rangle + |\rho\rangle)) \\
&= S(|\rho\rangle - (|x\rangle - |\text{init}\rangle + |\rho\rangle)) \\
&= |x\rangle + |\text{init}\rangle.
\end{aligned}$$

We can now prove that $|\kappa_x\rangle$ is a $(+1)$ -eigenvector,

$$U(\vec{\theta})(\mathbb{1} - 2|\overline{0, \text{init}}\rangle\langle\overline{0, \text{init}}|)(\mathbb{1} - 2|U_0\rangle\langle U_0|)|\kappa_x\rangle = |0, x\rangle + |0, \text{init}\rangle + \frac{1}{\sqrt{p_\tau}}|1, \tau\rangle = |\kappa_x\rangle.$$

To complete the proof, we show that $|\kappa_x\rangle$ is the *unique* $(+1)$ -eigenvector in \mathcal{H}_U . First, because $|\overline{0, \text{init}}\rangle$ is orthogonal to $|U_0\rangle$ by construction, the intermediate operator $U(\vec{\theta})(\mathbb{1} - 2|\overline{0, \text{init}}\rangle\langle\overline{0, \text{init}}|)$ has a $(+1)$ -eigenspace of two dimensions from Lemma 4, with one of the dimensions being $|U_0\rangle$. Second, the reflection of $|U_0\rangle$ reduces the dimensionality of the $(+1)$ -eigenspace by 1 by another application of Lemma 4, leaving the full operator with a unique $(+1)$ -eigenvector, which is $|\kappa_x\rangle$. \square

Lemma 6

$$\| |\kappa_x\rangle \|^2 = 2\text{HT}(\mathsf{P}, \vec{\pi} \rightarrow \vec{\tau}) - 2 \left\| \frac{\vec{\tau}}{\vec{\pi}} \cdot \vec{x} \right\|_1 + \frac{1 + p_\tau}{p_\tau}$$

where \cdot indicates entry-wise multiplication of vectors, and the division of vectors is also entry-wise.

Proof We use the fact that $|0, x\rangle$ and $|\overline{0, \text{init}}\rangle$ are orthogonal as proven above and find

$$\begin{aligned} \| |\kappa_x\rangle \|^2 &= \| |0, x\rangle \|^2 + \left\| \sqrt{\frac{1 + p_\tau}{p_\tau}} |\overline{0, \text{init}}\rangle \right\|^2 \\ &= \left(\frac{\vec{x}}{\sqrt{\vec{\pi}}} \right)^T \mathsf{T}^\dagger (\mathbb{1} - \mathsf{S})^2 \mathsf{T} \frac{\vec{x}}{\sqrt{\vec{\pi}}} + \frac{1 + p_\tau}{p_\tau} \\ &= 2 \left(\frac{\vec{x}}{\sqrt{\vec{\pi}}} \right)^T \frac{\vec{\pi} - \vec{\tau}}{\sqrt{\vec{\pi}}} + \frac{1 + p_\tau}{p_\tau} \\ &= 2 \|\vec{x}\|_1 - 2 \left\| \frac{\vec{\tau}}{\vec{\pi}} \cdot \vec{x} \right\|_1 + \frac{1 + p_\tau}{p_\tau} \\ &= 2\text{HT}(\mathsf{P}, \vec{\pi} \rightarrow \vec{\tau}) - 2 \left\| \frac{\vec{\tau}}{\vec{\pi}} \cdot \vec{x} \right\|_1 + \frac{1 + p_\tau}{p_\tau}. \end{aligned}$$

\square

We now prove our main result of the quadratic speed-up over access time in Theorem 7 and Corollary 8.

Theorem 7

$$\text{QHT}^2(U(\vec{\theta}), |0, \text{init}\rangle) = 2 \left(\frac{p_\tau}{1 + p_\tau} \right)^2 \left(\text{HT}(\mathsf{P}, \vec{\pi} \rightarrow \vec{\tau}) - \left\| \frac{\vec{\tau}}{\vec{\pi}} \cdot \vec{x} \right\|_1 \right)$$

Proof We prove the statement by using Equation 5.7 and identifying $|\kappa_{\text{un}}\rangle$ with $|\kappa_x\rangle$,

$$\begin{aligned} \text{QHT}^2(\text{U}(\vec{\theta}), |0, \text{init}\rangle) &= \frac{p_\tau}{1+p_\tau} \left(\frac{\|\kappa_x\|^2}{|\langle \kappa_x | 0, \text{init} \rangle|^2} - 1 \right) \\ &= \frac{p_\tau}{1+p_\tau} \left(\frac{2\text{HT}(\text{P}, \vec{\pi} \rightarrow \vec{\tau}) - 2\left\| \frac{\vec{\tau}}{\|\vec{\tau}\|} \cdot \vec{x} \right\|_1 + \frac{1+p_\tau}{p_\tau}}{\frac{1+p_\tau}{p_\tau}} - 1 \right) \\ &= 2 \left(\frac{p_\tau}{1+p_\tau} \right)^2 \left(\text{HT}(\text{P}, \vec{\pi} \rightarrow \vec{\tau}) - \left\| \frac{\vec{\tau}}{\|\vec{\tau}\|} \cdot \vec{x} \right\|_1 \right). \end{aligned}$$

□

Corollary 8 *Using $\text{U}(\vec{\theta})$ within phase estimation, we can generate an approximation of the state $|\tau\rangle$ with arbitrary precision from $|\text{init}\rangle$ with constant success probability using*

$$\Theta \left(\sqrt{\text{HT}(\text{P}, \vec{\pi} \rightarrow \vec{\tau}) - \left\| \frac{\vec{\tau}}{\|\vec{\tau}\|} \cdot \vec{x} \right\|_1} \right)$$

applications of $\text{U}(\vec{\theta})$.

Proof We set $p_\tau = 1$, which makes $|0, \text{init}\rangle$ an equal superposition of the $(+1)$ -eigenvector $|U_0\rangle$ and the orthogonal state $|\overline{0, \text{init}}\rangle$. Then, using Theorems 1 and 7, we can produce an approximation of $|U_0\rangle$ with $1/2$ probability in $\Theta \left(\sqrt{\text{HT}(\text{P}, \vec{\pi} \rightarrow \vec{\tau}) - \left\| \frac{\vec{\tau}}{\|\vec{\tau}\|} \cdot \vec{x} \right\|_1} \right)$ steps. We then measure the ancilla qubit: if it is $|1\rangle$ (with close to $1/2$ probability) then we have an approximation of the target state $|\tau\rangle$, and otherwise if it is $|0\rangle$ then we have an approximation of $|\text{init}\rangle$. Because of the nature of phase estimation, the larger the size of the phase estimation circuit, the closer we can approximate $|U_0\rangle$ and so the closer the resultant state will be to $|\tau\rangle$ when we succeed. □

5.1.1 Quantum Rejection Sampling

Consider the resampling problem from Section 1.1.1. In this problem, we have access to a black box that generates samples of a distribution $\vec{\sigma}$ which is strictly positive in all its elements, and we want to generate samples from a different probability distribution $\vec{\tau}$.

We can embed this into a random walk sampling problem, by letting P be the complete graph (including self-loops) with edge weights set to

$$w_{j \leftarrow i} = \sigma_j \sigma_i,$$

so that the transition probabilities are

$$P_{j \leftarrow i} = \frac{\sigma_j \sigma_i}{\sum_k \sigma_k \sigma_i} = \sigma_j.$$

Taking one step of P always results in an independent sample of $\vec{\sigma}$, so the stationary distribution of P is $\vec{\sigma}$. Since the edge weights are symmetric and $\sigma_i > 0$ for all i , P is reversible. Classical rejection sampling in this case is a local stopping rule with probabilities $\vec{q} = \gamma \frac{\tau_i}{\sigma_i}$, which makes the exit frequencies $\vec{x} = \frac{\vec{\sigma}}{\gamma} - \vec{\tau}$. The access time is $\gamma^{-1} - 1$, the expected number of steps for rejection sampling without counting the final accepted sample.

We can apply the results in Corollary 8 to this random walk with stopping rules that encode rejection sampling. We can then generate $|\tau\rangle$ using $\mathcal{O}(\sqrt{\gamma^{-1}})$ applications of $U(\vec{\theta})$ if we start in $|\text{init}\rangle = \sum_i \sqrt{\sigma_i} |i\rangle \otimes \sum_j \sqrt{\sigma_j} |j\rangle$. From Equation 4.2, the control angles satisfy $\cos(\theta_i) = (\frac{\sigma_i}{\tau_i} + 1)^{-1}$, and so we can compute them in superposition using a quantum implementation of a classical calculation, all without knowing a global property.

Ozols, Rötteler, and Roland [ORR13] gave a different quantum algorithm that builds on classical rejection sampling. Their algorithm encodes acceptance as $|1\rangle$ and rejection as $|0\rangle$ in an ancilla qubit. It performs amplitude amplification of the direct quantum analogue of classical rejection sampling, which provides a quadratic speed-up over the classical algorithm.

An advantage of the algorithm of Ozols, Rötteler, and Roland is that the amplitude amplification produces the exact target state $|\tau\rangle$, whereas using $U(\vec{\theta})$ within phase estimation produces an approximation of $|\tau\rangle$. An advantage of $U(\vec{\theta})$ is that it does not use the value of γ directly, since all of its calculations are local.

5.2 Starting in $|\overline{\text{init}}\rangle$

We can also use $U(\vec{\theta})$ when we limit the target distribution to a set of *marked vertices*, and start in $|\text{init}\rangle$ limited to the complement set of *unmarked vertices*. More precisely, we split the N vertices into the marked set \mathcal{M} and the complement unmarked set \mathcal{U} . Our initial state is then

$$|\overline{\text{init}}\rangle = \frac{1}{\sqrt{1-\varepsilon}} \sum_{i \in \mathcal{U}} \sqrt{\pi_i} |i, p_i\rangle \quad (5.14)$$

where

$$\varepsilon = \sum_{i \in \mathcal{M}} \pi_i \quad (5.15)$$

is the probability that a given classical sample of $\vec{\pi}$ is of a marked vertex. We use the subscripts \mathcal{U} and \mathcal{M} on vectors to limit the vectors to their unmarked and marked components (i.e. the subscript indicates setting the other component to zero, without renormalizing).

Similarly to how we decomposed $|\text{init}\rangle$ into its $|U_0\rangle$ component and an orthogonal component (Equation 5.5), we decompose $|0, \overline{\text{init}}\rangle$ into its $|U_0\rangle$ component and the component orthogonal to $|U_0\rangle$. To do this, we first rewrite $|U_0\rangle$ as

$$\begin{aligned} |U_0\rangle &= \frac{1}{\sqrt{1+p_\tau}} (|0, \text{init}\rangle - |1, \tau_{\text{un}}\rangle) \\ &= \frac{1}{\sqrt{1+p_\tau}} (|0\rangle \text{T} \sqrt{\vec{\pi}_{\mathcal{U}}} + |0\rangle \text{T} \sqrt{\vec{\pi}_{\mathcal{M}}} - |1\rangle \text{T} \sqrt{\vec{\tau}_{\text{un}}}) \\ &= \frac{1}{\sqrt{1+p_\tau}} \left(\sqrt{1-\varepsilon} |0, \overline{\text{init}}\rangle + \sum_{i \in \mathcal{M}} (\sqrt{\pi_i} |0\rangle - \sqrt{\tau_{\text{un},i}} |1\rangle) |i, p_i\rangle \right) \\ &= \frac{1}{\sqrt{1+p_\tau}} \left(\sqrt{1-\varepsilon} |0, \overline{\text{init}}\rangle - \sum_{i \in \mathcal{M}} \sqrt{\pi_i + \tau_{\text{un},i}} |\tilde{1}_i\rangle |i, p_i\rangle \right) \\ &= \frac{1}{\sqrt{1+p_\tau}} (\sqrt{1-\varepsilon} |0, \overline{\text{init}}\rangle - \sqrt{\varepsilon + p_\tau} |\widetilde{1, \tau}\rangle). \end{aligned} \quad (5.16)$$

We can express the normalized state $|\widetilde{1, \tau}\rangle$ introduced above in the equivalent formula-

tions

$$\begin{aligned}
|\widetilde{\mathbf{1}}, \tau\rangle &= \frac{1}{\sqrt{\varepsilon + p_\tau}} (-|0\rangle \mathbb{T} \sqrt{\vec{\pi}_{\mathcal{M}}} + |\mathbf{1}, \tau_{\text{un}}\rangle) \\
&= \frac{1}{\sqrt{\varepsilon + p_\tau}} \sum_{i \in \mathcal{M}} \sqrt{\pi_i + \tau_{\text{un},i}} |\tilde{\mathbf{1}}_i\rangle |i, p_i\rangle \\
&= \sum_{i \in \mathcal{M}} \sqrt{\tilde{\tau}_i} |\tilde{\mathbf{1}}_i\rangle |i, p_i\rangle
\end{aligned} \tag{5.17}$$

where in the last formulation we use the mixed distribution

$$\vec{\tau} = \frac{\vec{\pi}_{\mathcal{M}} + \vec{\tau}_{\text{un}}}{\varepsilon + p_\tau}. \tag{5.18}$$

We now determine the component of $|0, \overline{\text{init}}\rangle$ orthogonal to $|U_0\rangle$,

$$|U_+\rangle = \frac{1}{\sqrt{1 + p_\tau}} (\sqrt{\varepsilon + p_\tau} |0, \overline{\text{init}}\rangle + \sqrt{1 - \varepsilon} |\widetilde{\mathbf{1}}, \tau\rangle) \tag{5.19}$$

$$= \frac{(\varepsilon + p_\tau) |0\rangle \mathbb{T} \sqrt{\vec{\pi}} - \sqrt{1 - \varepsilon} (|0\rangle \mathbb{T} \sqrt{\vec{\pi}_{\mathcal{M}}} + |\mathbf{1}, \tau_{\text{un}}\rangle)}{\sqrt{(1 + p_\tau)(\varepsilon + p_\tau)}}. \tag{5.20}$$

Now consider the random walk with optimal stopping rules which begins in

$$\vec{\pi} = \frac{\vec{\pi}_{\mathcal{U}}}{1 - \varepsilon} \tag{5.21}$$

and ends in the mixed distribution $\vec{\tau}$. We denote the vector of exit frequencies for this walk as \vec{x} .

Lemma 9 *The unique (+1)-eigenvector of the operator*

$$\mathbb{U}(\vec{\theta})(\mathbb{1} - 2|U_+\rangle\langle U_+|)(\mathbb{1} - 2|U_0\rangle\langle U_0|)$$

in \mathcal{H}_U is

$$|\kappa_{\vec{x}}\rangle = |0, \vec{x}\rangle \tag{5.22}$$

where

$$|\vec{x}\rangle = (\mathbb{1} - \mathbb{S}) \mathbb{T} \frac{\vec{x}}{\sqrt{\vec{\pi}}}. \tag{5.23}$$

Proof Again, we show that $|0, \tilde{x}\rangle$ is a $(+1)$ -eigenvector by direct calculation. The first reflection is of $|U_0\rangle$, which is a superposition of $|0, \text{init}\rangle$ and $|1, \tau\rangle$. Since $|\text{init}\rangle$ is a $(+1)$ -eigenvector of S and $|\tilde{x}\rangle$ is a (-1) -eigenvector of S , it follows that $\langle U_0|0, \tilde{x}\rangle = 0$ so

$$(\mathbb{1} - 2|U_0\rangle\langle U_0|)|0, \tilde{x}\rangle = |0, \tilde{x}\rangle.$$

The second reflection is of $|U_+\rangle$. We first evaluate $T^\dagger|\tilde{x}\rangle$ using the analogous result to Equation 5.13,

$$\begin{aligned} T^\dagger|\tilde{x}\rangle &= \frac{\vec{\pi} - \vec{\tau}}{\sqrt{\pi}} \\ &= \sqrt{\frac{\vec{\pi}}{1-\varepsilon}} - \frac{\vec{\tau}}{\sqrt{\pi}}. \end{aligned} \tag{5.24}$$

The inner product of $|U_+\rangle$ and $|0, \tilde{x}\rangle$ is then

$$\begin{aligned} &\frac{\left((\varepsilon + p_\tau)\sqrt{\frac{\vec{\pi}}{\pi}} - \sqrt{1-\varepsilon}\sqrt{\frac{\vec{\tau}}{\pi}}\right)^T T^\dagger(\mathbb{1} - S)T \frac{\vec{x}}{\sqrt{\pi}}}{\sqrt{(1+p_\tau)(\varepsilon+p_\tau)}} \\ &= \frac{\left((\varepsilon + p_\tau)\sqrt{\frac{\vec{\pi}}{\pi}} - \sqrt{1-\varepsilon}\sqrt{\frac{\vec{\tau}}{\pi}}\right)^T \left(\sqrt{\frac{\vec{\pi}}{1-\varepsilon}} - \frac{\vec{\tau}}{\sqrt{\pi}}\right)}{\sqrt{(1+p_\tau)(\varepsilon+p_\tau)}} \\ &= \frac{\varepsilon + p_\tau + 1 - \varepsilon}{\sqrt{(1+p_\tau)(\varepsilon+p_\tau)(1-\varepsilon)}} \\ &= \sqrt{\frac{1+p_\tau}{(\varepsilon+p_\tau)(1-\varepsilon)}}, \end{aligned}$$

so applying the second reflection gives

$$\begin{aligned} &(\mathbb{1} - 2|U_+\rangle\langle U_+|)(\mathbb{1} - 2|U_0\rangle\langle U_0|)|0, \tilde{x}\rangle \\ &= |0, \tilde{x}\rangle - 2\sqrt{\frac{1+p_\tau}{(\varepsilon+p_\tau)(1-\varepsilon)}}|U_+\rangle \\ &= |0, \tilde{x}\rangle - \frac{2}{\sqrt{1-\varepsilon}}|0, \overline{\text{init}}\rangle - \frac{2}{\sqrt{\varepsilon+p_\tau}}|\widetilde{1, \tau}\rangle \\ &= |0, \tilde{x}\rangle - \frac{2}{\sqrt{1-\varepsilon}}|0, \overline{\text{init}}\rangle + \frac{2}{\varepsilon+p_\tau}|0\rangle T \sqrt{\frac{\vec{\tau}}{\pi}} - \frac{2}{\varepsilon+p_\tau}|1, \tau_{\text{un}}\rangle. \end{aligned} \tag{5.25}$$

We finally apply $U(\vec{\theta})$. The first stage of $U(\vec{\theta})$ consists of the N reflections of $|\vec{0}_i\rangle|i, p_i\rangle$. Noting the similarity between Equations 5.10 and 5.25, we use that the state $|0, \rho\rangle +$

$\frac{1}{\sqrt{p_\tau}}|1, \tau\rangle$, rescaled as

$$\frac{1}{\varepsilon + p_\tau}(p_\tau|0, \rho\rangle + |1, \tau_{\text{un}}\rangle),$$

is in the span of the reflected states. Using

$$\begin{aligned} \frac{1}{\varepsilon + p_\tau}|1, \tau_{\text{un}}\rangle &= \frac{1}{\sqrt{\varepsilon + p_\tau}}|\widetilde{1}, \tau\rangle + \frac{1}{\varepsilon + p_\tau}|0\rangle\mathbb{T}\sqrt{\vec{\pi}_{\mathcal{M}}} \\ \mathbb{T}\frac{\vec{\tau}}{\sqrt{\vec{\pi}}} &= \frac{2}{\varepsilon + p_\tau}\mathbb{T}\sqrt{\vec{\pi}_{\mathcal{M}}} - \frac{1}{\varepsilon + p_\tau}\mathbb{T}\sqrt{\vec{\pi}_{\mathcal{M}}} + \frac{p_\tau}{\varepsilon + p_\tau}|\rho\rangle, \end{aligned}$$

we rewrite our intermediate state as

$$\left(|0, \tilde{x}\rangle - \frac{2}{\sqrt{1-\varepsilon}}|0, \overline{\text{init}}\rangle + |0\rangle\mathbb{T}\frac{\vec{\tau}}{\sqrt{\vec{\pi}}} - \frac{1}{\sqrt{\varepsilon + p_\tau}}|\widetilde{1}, \tau\rangle\right) - \frac{1}{\varepsilon + p_\tau}(p_\tau|0, \rho\rangle + |1, \tau_{\text{un}}\rangle).$$

From $|\widetilde{1}, \tau\rangle = \sum_{i \in \mathcal{M}} \sqrt{\tilde{c}_i} |\tilde{1}_i\rangle |i, p_i\rangle$, the reflections do not affect $|\widetilde{1}, \tau\rangle$. From Equation 5.24, the term $|0, \tilde{x}\rangle - \frac{2}{\sqrt{1-\varepsilon}}|0, \overline{\text{init}}\rangle + |0\rangle\mathbb{T}\frac{\vec{\tau}}{\sqrt{\vec{\pi}}}$ is not in the image of \mathbb{T} so the reflections do not affect it either. Thus the reflections produce the state

$$\begin{aligned} &\left(|0, \tilde{x}\rangle - \frac{2}{\sqrt{1-\varepsilon}}|0, \overline{\text{init}}\rangle + |0\rangle\mathbb{T}\frac{\vec{\tau}}{\sqrt{\vec{\pi}}} - \frac{1}{\sqrt{\varepsilon + p_\tau}}|\widetilde{1}, \tau\rangle\right) + \frac{1}{\varepsilon + p_\tau}(p_\tau|0, \rho\rangle + |1, \tau_{\text{un}}\rangle) \\ &= |0\rangle\left(|\tilde{x}\rangle - \frac{2}{\sqrt{1-\varepsilon}}|\overline{\text{init}}\rangle + \mathbb{T}\frac{\vec{\tau}}{\sqrt{\vec{\pi}}} + \frac{\mathbb{T}\sqrt{\vec{\pi}_{\mathcal{M}}} + p_\tau|\rho\rangle}{\varepsilon + p_\tau}\right) + |1\rangle\frac{-|\tau_{\text{un}}\rangle + |\tau_{\text{un}}\rangle}{\varepsilon + p_\tau} \\ &= |0\rangle\left(|\tilde{x}\rangle - \frac{2}{\sqrt{1-\varepsilon}}|\overline{\text{init}}\rangle + 2\mathbb{T}\frac{\vec{\tau}}{\sqrt{\vec{\pi}}}\right). \end{aligned}$$

We now apply $W = S(2\mathbb{T}\mathbb{T}^\dagger - \mathbb{1})$ to the state $|\tilde{x}\rangle - \frac{2}{\sqrt{1-\varepsilon}}|\overline{\text{init}}\rangle + 2\mathbb{T}\frac{\vec{\tau}}{\sqrt{\vec{\pi}}}$,

$$S\left(\frac{2}{\sqrt{1-\varepsilon}}|\overline{\text{init}}\rangle - 2\mathbb{T}\frac{\vec{\tau}}{\sqrt{\vec{\pi}}} - |\tilde{x}\rangle - \frac{2}{\sqrt{1-\varepsilon}}|\overline{\text{init}}\rangle + 2\mathbb{T}\frac{\vec{\tau}}{\sqrt{\vec{\pi}}}\right) = |\tilde{x}\rangle,$$

where the last line follows from $|\tilde{x}\rangle$ being a (-1) -eigenvector of S .

We conclude this proof by proving the uniqueness of $|\kappa_{\tilde{x}}\rangle$ in \mathcal{H}_U (up to scalars). The unique $(+1)$ -eigenvector of $U(\vec{\theta})$ in \mathcal{H}_U is $|U_0\rangle$ by Lemma 3. Since $|U_+\rangle$ is orthogonal to $|U_0\rangle$, by Lemma 4, the operator $U(\vec{\theta})(\mathbb{1} - 2|U_+\rangle\langle U_+|)$ has two $(+1)$ -eigenvectors, one of which is $|U_0\rangle$. With the reflection of $|U_0\rangle$, the overall operator $U(\vec{\theta})(\mathbb{1} - 2|U_+\rangle\langle U_+|)(\mathbb{1} - 2|U_0\rangle\langle U_0|)$ has a unique $(+1)$ -eigenvector in \mathcal{H}_U . From the above it is $|\kappa_{\tilde{x}}\rangle = |0, \tilde{x}\rangle$. \square

Lemma 10

$$\|\kappa_{\tilde{x}}\|^2 = \frac{2}{1-\varepsilon} \|\tilde{x}_{\mathcal{U}}\|_1 - 2 \left\| \tilde{\tau} \cdot \frac{\tilde{x}}{\tilde{\pi}} \right\|_1 \quad (5.26)$$

Proof

$$\begin{aligned} \|\kappa_{\tilde{x}}\|^2 &= \|\tilde{x}\|^2 \\ &= \langle \tilde{x} | \tilde{x} \rangle \\ &= 2 \left(\frac{\tilde{x}}{\sqrt{\tilde{\pi}}} \right)^T (\mathbb{T}^\dagger (\mathbb{1} - \mathbb{S}) \mathbb{T}) \left(\frac{\tilde{x}}{\sqrt{\tilde{\pi}}} \right) \\ &= 2 \left(\frac{\tilde{x}}{\sqrt{\tilde{\pi}}} \right)^T \left(\frac{\tilde{\pi} - \tilde{\tau}}{\sqrt{\tilde{\pi}}} \right) \\ &= 2 \left(\frac{\tilde{x}}{\sqrt{\tilde{\pi}}} \right)^T \left(\frac{\sqrt{\tilde{\pi}_{\mathcal{U}}}}{1-\varepsilon} - \frac{\tilde{\tau}}{\sqrt{\tilde{\pi}}} \right) \\ &= \frac{2}{1-\varepsilon} \|\tilde{x}_{\mathcal{U}}\|_1 - 2 \left\| \tilde{\tau} \cdot \frac{\tilde{x}}{\tilde{\pi}} \right\|_1. \end{aligned}$$

□

We now prove that we can sample from $|\tau\rangle$ starting from $|\overline{\text{init}}\rangle$ quadratically faster than using random walks and stopping rules to sample the mixed distribution $\tilde{\tau}$ after starting from $\tilde{\pi}$.

Theorem 11

$$\text{QHT}_{\text{cot}}^2(\mathbb{U}(\vec{\theta}), |0, \overline{\text{init}}\rangle) = 2 \left(\frac{\varepsilon + p_\tau}{1 + p_\tau} \right)^2 \left(\text{HT}(\mathbb{P}, \tilde{\pi} \rightarrow \tilde{\tau}) - \delta \right) \quad (5.27)$$

where

$$\delta = (1-\varepsilon) \left\| \tilde{\tau} \cdot \frac{\tilde{x}}{\tilde{\pi}} \right\|_1 + \|\tilde{x}_{\mathcal{M}}\|_1 + \frac{1}{2} \frac{1 + p_\tau}{\varepsilon + p_\tau}. \quad (5.28)$$

Proof

$$\begin{aligned}
\text{QHT}_{\text{cot}}^2(\text{U}(\vec{\theta}), |0, \overline{\text{init}}\rangle) &= \text{QHT}_{\text{cot}}^2\left(\text{U}(\vec{\theta}), \frac{1}{\sqrt{1+p_\tau}}(\sqrt{1-\varepsilon}|U_0\rangle + \sqrt{\varepsilon+p_\tau}|U_+\rangle)\right) \\
&= \frac{\varepsilon+p_\tau}{1+p_\tau} \text{QHT}_{\text{cot}}^2(\text{U}(\vec{\theta}), |U_+\rangle) \\
&= \frac{\varepsilon+p_\tau}{1+p_\tau} \left(\frac{\|\kappa_{\vec{x}}\|^2}{|\langle \vec{\kappa} | U_+\rangle|^2} - 1 \right) \\
&= \frac{\varepsilon+p_\tau}{1+p_\tau} \left(\frac{\frac{2}{1-\varepsilon} \|\vec{x}_{\mathcal{U}}\|_1 - 2 \|\vec{\tau} \cdot \frac{\vec{x}}{\vec{\pi}}\|_1}{\frac{1+p_\tau}{(1-\varepsilon)(\varepsilon+p_\tau)}} - 1 \right) \\
&= 2 \left(\frac{\varepsilon+p_\tau}{1+p_\tau} \right)^2 \left(\|\vec{x}_{\mathcal{U}}\|_1 - (1-\varepsilon) \left\| \vec{\tau} \cdot \frac{\vec{x}}{\vec{\pi}} \right\|_1 - \frac{1+p_\tau}{2\varepsilon+p_\tau} \right) \\
&= 2 \left(\frac{\varepsilon+p_\tau}{1+p_\tau} \right)^2 \left(\text{HT}(\text{P}, \vec{\pi} \rightarrow \vec{\tau}) - \delta \right)
\end{aligned}$$

where in the last step we use Equation 5.28 together with

$$\text{HT}(\text{P}, \vec{\pi} \rightarrow \vec{\tau}) = \|\vec{x}\|_1 = \|\vec{x}_{\mathcal{U}}\|_1 + \|\vec{x}_{\mathcal{M}}\|_1.$$

□

Corollary 12 *When $\varepsilon < 1/2$, we can use $\text{U}(\vec{\theta})$ within phase estimation to generate an approximation of the state $|\tau\rangle$ with arbitrary precision from $|\overline{\text{init}}\rangle$ with constant success probability using*

$$\mathcal{O}\left(\sqrt{\text{HT}(\text{P}, \vec{\pi} \rightarrow \vec{\tau})}\right)$$

applications of $\text{U}(\vec{\theta})$.

Proof Here we set $p_\tau = 1 - 2\varepsilon$, which makes $|0, \overline{\text{init}}\rangle$ an equal superposition of the $(+1)$ -eigenvector $|U_0\rangle$ and of $|\widetilde{1}, \tau\rangle$. Then, using Theorems 1 and 11, we can produce an approximation of $|U_0\rangle$ with $1/2$ probability in $\mathcal{O}\left(\sqrt{\text{HT}(\text{P}, \vec{\pi} \rightarrow \vec{\tau})}\right)$ steps.

Once we have this approximation of $|U_0\rangle$, the steps to produce an approximation of $|\tau\rangle$ are identical to Corollary 8, except that the probability to measure $|1\rangle$ from $|U_0\rangle$ becomes

$$\frac{p_\tau}{1+p_\tau} = \frac{1-2\varepsilon}{2-2\varepsilon}$$

which approaches $1/2$ as ε approaches 0. □

Chapter 6

Interpolated Walks

6.1 Construction

Krovi, Magniez, Ozols, and Roland [KMOR16] introduced and analyzed the *interpolated walk*, which interpolates between a random walk P and a walk where marked vertices are absorbing, so their only outgoing edge is a self-loop. We extend their construction by allowing a different interpolation parameter for each vertex on the graph. Formally, given an irreducible random walk P (so that the stationary distribution is unique), we can construct an interpolated walk by adding self-loops \vec{s} to each vertex,

$$P(\vec{s}) = P \operatorname{diag}(1 - \vec{s}) + \operatorname{diag}(\vec{s}). \quad (6.1)$$

Taking one step of the walk $P(\vec{s})$ when in vertex i consists of remaining in vertex i with probability s_i and taking a step of P with probability $1 - s_i$. These self-loops thus allow us to modify the stationary distribution to (up to normalization)

$$\vec{\pi}_s = \frac{\vec{\pi}}{1 - \vec{s}}. \quad (6.2)$$

We show this by calculation,

$$\begin{aligned} P(\vec{s})\vec{\pi}_s &= P \operatorname{diag}(1 - \vec{s}) \frac{\vec{\pi}}{1 - \vec{s}} + \operatorname{diag}(\vec{s}) \frac{\vec{\pi}}{1 - \vec{s}} \\ &= \left(1 + \frac{\vec{s}}{1 - \vec{s}}\right) \vec{\pi} \\ &= \frac{\vec{\pi}}{1 - \vec{s}} \\ &= \vec{\pi}_s. \end{aligned}$$

6.2 Sampling From Interpolated Walks

Interpolated walks operate by modifying the stationary distribution of a random walk, unlike classical stopping rules which have a well-defined stopping condition. Classical sampling using interpolated walks thus consists of approaching the modified stationary distribution from the initial distribution.

If our goal is to sample from $\vec{\tau}$, then we set the self-loops so that the new stationary distribution is the mixed distribution $\vec{\pi} + \vec{\tau}_{\text{un}}$,

$$\begin{aligned}\vec{\pi} + \vec{\tau}_{\text{un}} &= \frac{\vec{\pi}}{1 - \vec{s}} \\ \vec{s} &= 1 - \frac{\vec{\pi}}{\vec{\pi} + \vec{\tau}_{\text{un}}} = \frac{\vec{\tau}_{\text{un}}}{\vec{\pi} + \vec{\tau}_{\text{un}}}.\end{aligned}\tag{6.3}$$

Once we have run the walk for a sufficiently long time so that we have reached a close approximation of the new stationary distribution $\vec{\pi}_s$, we then take one more step of the walk. If we take the self-loop in this final step, then we have sampled from

$$\vec{\pi}_s \cdot \vec{s} = (\vec{\pi} + \vec{\tau}_{\text{un}}) \cdot \frac{\vec{\tau}_{\text{un}}}{\vec{\pi} + \vec{\tau}_{\text{un}}} = \vec{\tau}_{\text{un}}$$

which is the target distribution. If we do not take the self-loop, then we have sampled from

$$\vec{\pi}_s \cdot (1 - \vec{s}) = (\vec{\pi} + \vec{\tau}_{\text{un}}) \cdot \frac{\vec{\pi}}{\vec{\pi} + \vec{\tau}_{\text{un}}} = \vec{\pi}$$

which is the stationary distribution of the original walk P , at which point we could run the interpolated walk again, using a similar idea to rejection sampling.

Note the close resemblance between classical sampling using interpolated walks and using the controlled quantum walk: taking the self-loop resembles seeing $|1\rangle$ in the ancilla qubit and not applying W , and not taking it resembles seeing $|0\rangle$ and applying W . This hints at the equivalence explained in the next section.

6.3 Embedding Quantum Interpolated Walks Into Controlled Quantum Walks

The quantum interpolated walk $W(\vec{s})$ is the construction of W as described in Section 3.3 applied to $P(\vec{s})$. One important difference is that we consider the new self-loops added by \vec{s} as *new* edges on the graph, as opposed to an increased weight of possibly pre-existing self-loops. If we use normalized edge weights (so that $\sum_{i,j} w_{j \leftarrow i} = 1$), then the added self-loops have weight

$$\begin{aligned} w_{i \circ} &= \frac{s_i}{1 - s_i} \sum_j w_{j \leftarrow i} \\ &= \frac{s_i}{1 - s_i} \pi_i \\ &= \frac{\tau_{\text{un},i}}{\pi_i} \pi_i \\ &= \tau_{\text{un},i}. \end{aligned}$$

As distinct edges, they also correspond to distinct quantum states. We denote these new states as $|i^\circ\rangle$, and they satisfy

$$\begin{aligned} T^\dagger |i^\circ\rangle &= 0 \\ S |i^\circ\rangle &= |i^\circ\rangle. \end{aligned}$$

The states $|i, p(\vec{s})_i\rangle = T(\vec{s})|i\rangle$ decompose as

$$|i, p(\vec{s})_i\rangle = \sqrt{1 - s_i} |i, p_i\rangle + \sqrt{s_i} |i^\circ\rangle. \quad (6.4)$$

There is an isometry that takes quantum interpolated walks to controlled quantum walks, and using this isometry we can embed the former into the latter. The isometry we present extends the discussion by Dohotaru and Høyer [DH17] to the case of different self-loops (for quantum interpolated walks) and angles (for controlled quantum walks) for each vertex.

The key ideas of the isometry are, first, that the new self-loops added by \vec{s} correspond to a value of $|1\rangle$ in the ancilla qubit as follows,

$$\begin{aligned} E|i, j\rangle &= |0\rangle|i, j\rangle \\ E|i^\circ\rangle &= -|1\rangle|i, p_i\rangle. \end{aligned} \tag{6.5}$$

Second, we set the angles of $U(\vec{\theta})$ so that

$$\cos^2(\vec{\theta}) = \vec{s}. \tag{6.6}$$

We can see from Equation 6.5 that orthogonal states map to orthogonal states, and so E preserves inner products, proving that it is an isometry. E is thus an embedding from the $(N^2 + N)$ -dimensional walk space with added self-loops to the $(2N^2)$ -dimensional walk space without self-loops and with the ancilla qubit.

By Equation 6.4, the embedding takes the space $\mathcal{H}_{W(\vec{s})}$ to the space \mathcal{H}_U , as we can see by applying it to states in the image of $T(\vec{s})$ and $ST(\vec{s})$,

$$\begin{aligned} E|i, p(\vec{s})_i\rangle &= \sqrt{1 - s_i}|0\rangle|i, p_i\rangle - \sqrt{s_i}|1\rangle|i, p_i\rangle \\ E|p(\vec{s})_i, i\rangle &= \sqrt{1 - s_i}|0\rangle|p_i, i\rangle - \sqrt{s_i}|1\rangle|i, p_i\rangle. \end{aligned} \tag{6.7}$$

We now show that quantum interpolated walks behave in the same way as controlled quantum walks.

Theorem 13 *Applying the quantum interpolated walk before the isometry is equal to applying the isometry before the controlled quantum walk, i.e.*

$$E W(\vec{s}) = U(\vec{\theta}) E. \tag{6.8}$$

Proof We prove Equation 6.8 by showing that the two operators have the same effect on basis states of the space of edges and added self-loops. First, we show this holds for the

added self-loop states $|i^\circ\rangle$,

$$\begin{aligned}
E W(\vec{s})|i^\circ\rangle &= E S(T(\vec{s})T(\vec{s})^\dagger - \mathbb{1})|i^\circ\rangle \\
&= E(2|p(\vec{s})_i, i\rangle\langle i, p(\vec{s})_i|i^\circ\rangle - |i^\circ\rangle) \\
&= E(2\sqrt{s_i}|p(\vec{s})_i, i\rangle - |i^\circ\rangle) \\
&= 2\sqrt{s_i(1-s_i)}|0\rangle|p_i, i\rangle - 2s_i|1\rangle|i, p_i\rangle + |1\rangle|i, p_i\rangle \\
&= 2\sqrt{s_i(1-s_i)}|0\rangle|p_i, i\rangle + (1-2s_i)|1\rangle|i, p_i\rangle \\
U(\vec{\theta}) E|i^\circ\rangle &= -U(\vec{\theta})|1\rangle|i, p_i\rangle \\
&= -(|0\rangle\langle 0| \otimes W + |1\rangle\langle 1| \otimes \mathbb{1})(|1\rangle - 2|\tilde{0}_i\rangle\langle \tilde{0}_i|1\rangle)|i, p_i\rangle \\
&= -(|0\rangle\langle 0| \otimes W + |1\rangle\langle 1| \otimes \mathbb{1})(|1\rangle - 2\sqrt{1-s_i}|\tilde{0}_i\rangle)|i, p_i\rangle \\
&= (|0\rangle\langle 0| \otimes W + |1\rangle\langle 1| \otimes \mathbb{1})(2\sqrt{s_i(1-s_i)}|0\rangle + (1-2s_i)|1\rangle)|i, p_i\rangle \\
&= 2\sqrt{s_i(1-s_i)}|0\rangle|p_i, i\rangle + (1-2s_i)|1\rangle|i, p_i\rangle.
\end{aligned}$$

Second, we show this holds for the states of the form $|i, j\rangle$,

$$\begin{aligned}
E W(\vec{s})|i, j\rangle &= E S(T(\vec{s})T(\vec{s})^\dagger - \mathbb{1})|i, j\rangle \\
&= E(2|p(\vec{s})_i, i\rangle\langle i, p(\vec{s})_i|i, j\rangle - |j, i\rangle) \\
&= E\left(2\sqrt{P_{j\leftarrow i}(1-s_i)}|p(\vec{s})_i, i\rangle - |j, i\rangle\right) \\
&= 2\sqrt{P_{j\leftarrow i}(1-s_i)}|0\rangle|p_i, i\rangle - |0\rangle|j, i\rangle - 2\sqrt{P_{j\leftarrow i}s_i(1-s_i)}|1\rangle|i, p_i\rangle \\
U(\vec{\theta}) E|i, j\rangle &= U(\vec{\theta})|0\rangle|i, j\rangle \\
&= (|0\rangle\langle 0| \otimes W + |1\rangle\langle 1| \otimes \mathbb{1})(|0\rangle|i, j\rangle - 2|\tilde{0}_i, i, p_i\rangle\langle \tilde{0}_i, i, p_i|0, i, j\rangle) \\
&= (|0\rangle\langle 0| \otimes W + |1\rangle\langle 1| \otimes \mathbb{1})(|0\rangle|i, j\rangle - 2\sqrt{P_{j\leftarrow i}s_i}|\tilde{0}_i, i, p_i\rangle) \\
&= 2\sqrt{P_{j\leftarrow i}}|0\rangle|p_i, i\rangle - |0\rangle|j, i\rangle - 2\sqrt{P_{j\leftarrow i}}\left(s_i|0\rangle|p_i, i\rangle + \sqrt{s_i(1-s_i)}|1\rangle|i, p_i\rangle\right) \\
&= 2\sqrt{P_{j\leftarrow i}(1-s_i)}|0\rangle|p_i, i\rangle - |0\rangle|j, i\rangle - 2\sqrt{P_{j\leftarrow i}s_i(1-s_i)}|1\rangle|i, p_i\rangle.
\end{aligned}$$

□

6.4 Extended Hitting Time

The original quantum interpolated walk as introduced by Krovi, Magniez, Ozols, and Roland [KMOR16] adds self-loops to the random walk P such that every vertex either has no added self-loop or has a self-loop of a single parameter s . It therefore splits the graph into marked and unmarked vertices, as discussed in Section 5.2. They expressed their results by introducing the *extended hitting time*, which in our framework maps to

$$\begin{aligned} \text{HT}^+(P, \mathcal{M}) &= \frac{(1 - s(1 - \varepsilon))^2}{\varepsilon^2} \text{HT}(\vec{s}) \\ &= \frac{(1 - s(1 - \varepsilon))^2}{2\varepsilon^2} \left(\text{QHT}^2(W(\vec{s}), |\overline{\text{init}}\rangle) + \frac{1 - \varepsilon}{1 + p_\tau} \right) \\ &= \frac{(1 - s(1 - \varepsilon))^2}{2\varepsilon^2} \left(\text{QHT}^2(U(\vec{\theta}), |0, \overline{\text{init}}\rangle) + \frac{1 - \varepsilon}{1 + p_\tau} \right). \end{aligned}$$

When the self-loops (and angles for $U(\vec{\theta})$) satisfy $\vec{\tau}_{\text{un}} = \frac{1-2\varepsilon}{\varepsilon} \vec{\pi}_{\mathcal{M}}$, i.e.

$$s = \frac{\tau_{\text{un},i}}{\tau_{\text{un},i} + \pi_i} = \frac{\frac{1-2\varepsilon}{\varepsilon}}{\frac{1-2\varepsilon}{\varepsilon} + \frac{1-\varepsilon}{\varepsilon}} = \frac{1-2\varepsilon}{1-\varepsilon},$$

which also sets $p_\tau = 1 - 2\varepsilon$, we can simplify the extended hitting time further to

$$\text{HT}^+(P, \mathcal{M}) = 2\text{QHT}^2(U(\vec{\theta}), |0, \overline{\text{init}}\rangle) + 1.$$

Using the isometry, this angle matches the angle $\tilde{\theta}$ used by Dohotaru and Høyer [DH17].

From Theorem 11, we have that

$$\begin{aligned} &\text{QHT}_{\text{cot}}^2(U(\vec{\theta}), |0, \overline{\text{init}}\rangle) \\ &= 2 \left(\frac{\varepsilon + p_\tau}{1 + p_\tau} \right)^2 \left(\text{HT}(P, \vec{\pi} \rightarrow \vec{\tau}) - (1 - \varepsilon) \left\| \vec{\tau} \cdot \frac{\vec{x}}{\vec{\pi}} \right\|_1 - \|\vec{x}_{\mathcal{M}}\|_1 - \frac{1}{2} \frac{1 + p_\tau}{\varepsilon + p_\tau} \right) \\ &= 2 \left(\frac{1 - \varepsilon}{2 - 2\varepsilon} \right)^2 \left(\text{HT}(P, \vec{\pi} \rightarrow \vec{\pi}_{\mathcal{M}}/\varepsilon) - (1 - \varepsilon) \left\| \frac{\vec{\pi}_{\mathcal{M}}}{\varepsilon} \cdot \frac{\vec{x}}{\vec{\pi}} \right\|_1 - \|\vec{x}_{\mathcal{M}}\|_1 - \frac{1}{2} \frac{2 - 2\varepsilon}{1 - \varepsilon} \right) \\ &= \frac{1}{2} \left(\text{HT}(P, \vec{\pi} \rightarrow \vec{\pi}_{\mathcal{M}}/\varepsilon) - \frac{1}{\varepsilon} \|\vec{x}_{\mathcal{M}}\|_1 - 1 \right) \end{aligned}$$

so that we can express the extended hitting time as a function of access time by

$$\text{HT}^+(P, \mathcal{M}) = \text{HT}(P, \vec{\pi} \rightarrow \vec{\pi}_{\mathcal{M}}/\varepsilon) - \frac{1}{\varepsilon} \|\vec{x}_{\mathcal{M}}\|_1. \quad (6.9)$$

Chapter 7

Conclusion

We present the first quantum algorithm that can sample from any probability distribution over graph vertices. For any classical distribution $\vec{\tau}$ over vertices of a reversible random walk, our algorithm produces the corresponding quantum state $|\tau\rangle$. We prove that it has a quadratic speed-up over random walks with stopping rules.

Our work is the first use of random walks with stopping rules in the study of quantum walks. Our quantum algorithm generalizes the controlled quantum walk by Dohotaru and Høyer [DH17].

As we discuss in Section 4.1, we allow multiple control angles depending on the graph vertex, using the local formula

$$\cos^2(\theta_i) = \frac{\tau_i}{\pi_i + \tau_i} = \left(\frac{\pi_i}{\tau_i} + 1 \right)^{-1},$$

where $\vec{\pi}$ is the stationary distribution of the underlying random walk P .

We show in Theorems 7 and 11 that the quantum hitting time of this new algorithm $U(\vec{\theta})$ is quadratically smaller than the classical access time. The vector of exit frequencies \vec{x} , which encodes the expected number of times a random walk starting according to $\vec{\pi}$ will exit each vertex before stopping according to $\vec{\tau}$, connects the classical access time with the quantum hitting time. It is a single mathematical object that encodes within it the history of the walk, and as such it encodes information about the classical and quantum hitting times.

In Section 6.3, we give an isometry between quantum interpolated walks and our controlled quantum walk with multiple angles. We can thus embed the quantum analogue of a random walk with different self-loops added to each vertex into our controlled walk model with multiple angles.

In Section 6.4, we derive a new expression in Equation 6.9 for the extended hitting time, a quantity used in the study of interpolated quantum walks and controlled quantum walks. We show that the extended hitting time is a simple function of the exit frequencies of a random walk with a stopping rule that generates the stationary distribution limited to a set of marked nodes, after starting according to the stationary distribution limited to the complement set of unmarked nodes.

Exit frequencies and their quantum analogue $|x\rangle$ (defined in Equation 5.8) provide a new and exact mathematical link between classical and quantum algorithms for sampling over graph vertices. Their study reveals a new way to think about both algorithms and to prove relationships between them.

Bibliography

- [AA03] Scott Aaronson and Andris Ambainis. Quantum search of spatial regions. In *Proceedings of the 44th IEEE Symposium on Foundations of Computer Science, FOCS'03*, pages 200–209, 2003. arXiv:quant-ph/0303041, doi:10.1109/SFCS.2003.1238194.
- [AGJK20] Andris Ambainis, András Gilyén, Stacey Jeffery, and Mārtiņš Kokainis. Quadratic speedup for finding marked vertices by quantum walks, January 2020. Presented at the 23rd Annual Conference on Quantum Information Processing, QIP'20, Shenzhen, China.
- [AKR05] Andris Ambainis, Julia Kempe, and Alexander Rivosh. Coins make quantum walks faster. In *Proceedings of the 16th Annual ACM-SIAM Symposium on Discrete Algorithms, SODA'05*, pages 1099–1108, 2005. URL: <http://dl.acm.org/citation.cfm?id=1070432.1070590>, arXiv:quant-ph/0402107.
- [Amb04] Andris Ambainis. Quantum walk algorithm for element distinctness. In *Proceedings of the 45th IEEE Symposium on Foundations of Computer Science, FOCS'04*, pages 22–31, 2004. arXiv:quant-ph/0311001, doi:10.1109/FOCS.2004.54.
- [AS19] Simon Apers and Alain Sarlette. Quantum fast-forwarding: Markov chains and graph property testing. *Quantum Information & Computation*, 19(3–4):181–213, March 2019. doi:10.26421/QIC19.3-4.
- [BHMT02] Gilles Brassard, Peter Høyer, Michele Mosca, and Alain Tapp. Quantum amplitude amplification and estimation. In *Quantum Computation and Information*, volume 305 of *AMS Contemporary Mathematics*, pages 53–74. American Mathematical Society, 2002. arXiv:quant-ph/0005055.

- [CEMM98] Richard Cleve, Artur Ekert, Chiara Macchiavello, and Michele Mosca. Quantum algorithms revisited. *Proceedings of the Royal Society of London A: Mathematical, Physical and Engineering Sciences*, 454(1969):339–354, 1998. arXiv:quant-ph/9708016, doi:10.1098/rspa.1998.0164.
- [DH17] Cătălin Dohotaru and Peter Høyer. Controlled quantum amplification. In *Proceedings of the 44th International Colloquium on Automata, Languages, and Programming*, volume 80 of *ICALP'17*, pages 18:1–18:13, Dagstuhl, Germany, July 2017. Schloss Dagstuhl–Leibniz-Zentrum für Informatik. doi:10.4230/LIPIcs.ICALP.2017.18.
- [Doh15] Cătălin Dohotaru. *Efficient framework for quantum walks and beyond*. PhD thesis, University of Calgary, Calgary, Canada, December 2015. URL: <http://hdl.handle.net/11023/2700>.
- [dW16] Ronald de Wolf. Quantum computing: Lecture notes, May 2016. An introduction to quantum computing. URL: <http://homepages.cwi.nl/~rdewolf/qcnotes.pdf>.
- [Fro12] Ferdinand Georg Frobenius. Über matrizen aus nicht negativen elementen. *Sitzungsberichte der Königlich Preussischen Akademie der Wissenschaften*, pages 456–477, May 1912.
- [Gro96] Lov K. Grover. A fast quantum mechanical algorithm for database search. In *Proceedings of the 28th Annual ACM Symposium on Theory of Computing*, STOC'96, pages 212–219, 1996. arXiv:quant-ph/9605043, doi:10.1145/237814.237866.
- [Has70] Wilfred K. Hastings. Monte Carlo sampling methods using Markov chains and their applications. *Biometrika*, 57(1):97–109, April 1970. arXiv:<http://>

oup.prod.sis.lan/biomet/article-pdf/57/1/97/23940249/57-1-97.pdf,
doi:10.1093/biomet/57.1.97.

- [HdW02] Peter Høyer and Ronald de Wolf. Improved quantum communication complexity bounds for disjointness and equality. In *Proceedings of the 19th Symposium on Theoretical Aspects of Computer Science, STACS'02*, pages 299–310, 2002. arXiv:quant-ph/0109068, doi:10.1007/3-540-45841-7_24.
- [KMOR16] Hari Krovi, Frédéric Magniez, Māris Ozols, and Jérémie Roland. Quantum walks can find a marked element on any graph. *Algorithmica*, 74(2):851–907, 2016. arXiv:1002.2419, doi:10.1007/s00453-015-9979-8.
- [Lov93] László Lovász. Random walks on graphs: A survey. *Combinatorics, Paul Erdős is Eighty*, 1, 2:1–46, 1993. URL: <http://www.bolyai.hu/volumes.htm>.
- [LW95] László Lovász and Peter Winkler. Efficient stopping rules for Markov chains. In *Proceedings of the 27th Annual ACM Symposium on Theory of Computing, STOC'95*, pages 76–82, New York, NY, USA, June 1995. Association for Computing Machinery (ACM). doi:10.1145/225058.225086.
- [Mer07] N. David Mermin. *Quantum Computer Science: An Introduction*. Cambridge University Press, August 2007. doi:10.1017/CB09780511813870.
- [MRR⁺53] Nicholas Metropolis, Arianna W. Rosenbluth, Marshall N. Rosenbluth, Augusta H. Teller, and Edward Teller. Equation of state calculations by fast computing machines. *Journal of Chemical Physics*, 21(6):1087–1092, 1953.
- [ORR13] Māris Ozols, Martin Rötteler, and Jérémie Roland. Quantum rejection sampling. *ACM Transactions on Computation Theory*, 5(3):11:1–33, August 2013. doi:10.1145/2493252.2493256.

- [Per07] Oskar Perron. Zur theorie der matrices. *Mathematische Annalen*, 64(2):248–263, 1907.
- [Sze04] Mario Szegedy. Quantum speed-up of Markov chain based algorithms. In *Proceedings of the 45th IEEE Symposium on Foundations of Computer Science, FOCS'04*, pages 32–41, 2004. doi:10.1109/FOCS.2004.53.
- [Tul12] Avatar Tulsi. General framework for quantum search algorithms. *Physical Review A: General Physics*, 86(4):042331, October 2012. doi:10.1103/PhysRevA.86.042331.
- [vN51] John von Neumann. Various techniques used in connection with random digits. In A.S. Householder, G.E. Forsythe, and H.H. Germond, editors, *Monte Carlo Method*, pages 36–38. National Bureau of Standards Applied Mathematics Series, 12, Washington, D.C.: U.S. Government Printing Office, 1951.

Appendix A

Proof of the Flip-Flop Lemma

We adapt this proof from Dohotaru [Doh15], and adapt Lemma 14 from Tulsi [Tul12].

Let A be real unitary operator and let $|\psi\rangle$ be a real state, both in a state space \mathcal{H} . Let d be the number of positive/negative pairs of *distinct* eigenphases of A , where we count phases of 0 and π once each if they occur (from the complex conjugate root theorem, all eigenphases other than 0 and π come in positive/negative pairs). Sort the eigenphases as $-\pi \leq -\alpha_d < -\alpha_{d-1} < \dots < -\alpha_1 \leq 0 \leq \alpha_1 < \alpha_2 \leq \dots < \alpha_d \leq \pi$. For each eigenphase $\pm\alpha_j$, let $|\alpha_{j,\text{un}}^\pm\rangle$ be the unnormalized projection of $|\psi\rangle$ onto the associated eigenspace of A . The span of all the non-zero states $|\alpha_{j,\text{un}}^\pm\rangle$ then forms the space $\mathcal{H}_{|\psi\rangle}$.

Lemma 14 *Outside of $\mathcal{H}_{|\psi\rangle}$, the operator $A' = A(\mathbb{1} - 2|\psi\rangle\langle\psi|)$ behaves identically to A . Inside of $\mathcal{H}_{|\psi\rangle}$, the eigenphases of A' strictly interleave the eigenphases of A , so that there is a unique eigenphase of A' in between each consecutive pair of eigenphases of A along the unit circle.*

Proof [Tul12] Since $|\psi\rangle \in \mathcal{H}_{|\psi\rangle}$, the reflection $(1 - 2|\psi\rangle\langle\psi|)$ has no effect outside of $\mathcal{H}_{|\psi\rangle}$ so the operators A and A' behave identically outside of $\mathcal{H}_{|\psi\rangle}$. In particular, this means that all the eigenvectors of A' lie either entirely inside or entirely outside $\mathcal{H}_{|\psi\rangle}$. The remainder of the proof considers only the space $\mathcal{H}_{|\psi\rangle}$.

We find the relationship between the spectra of A and A' by finding the inner product between their eigenvectors, among those which lie in $\mathcal{H}_{|\psi\rangle}$. Let $|\alpha_j^+\rangle$ be an eigenvector of A in $\mathcal{H}_{|\psi\rangle}$ with eigenvalue α_j , and let $|\beta_j^+\rangle$ be an eigenvector of A' in $\mathcal{H}_{|\psi\rangle}$ with eigenphase β_j . For the eigenvectors of A or A' in $\mathcal{H}_{|\psi\rangle}$ with negative eigenphases, the below follows equivalently by negating the relevant eigenphase, so the choice of positive eigenphases

does not lose generality.

$$\begin{aligned}
e^{i\beta_k} \langle \alpha_j^+ | \beta_k \rangle &= \langle \alpha_j^+ | A' | \beta_k \rangle \\
&= e^{+i\alpha_j} \langle \alpha_j^+ | (|\beta_k\rangle - 2|\psi\rangle\langle\psi|\beta_k\rangle) \\
&= e^{+i\alpha_j} (\langle \alpha_j^+ | \beta_k \rangle - 2\langle \alpha_j^+ | \psi \rangle \langle \psi | \beta_k \rangle) \\
\langle \alpha_j^+ | \beta_k \rangle &= \frac{2}{1 - e^{i(\beta_k - \alpha_j)}} \langle \alpha_j^+ | \psi \rangle \langle \psi | \beta_k \rangle.
\end{aligned}$$

Since $|\psi\rangle$ lies in $\mathcal{H}_{|\psi\rangle}$, we can write the inner product of $|\psi\rangle$ with $|\beta_k\rangle$ and add the identity within $\mathcal{H}_{|\psi\rangle}$ composed of eigenvectors $|\alpha_j^\pm\rangle$ of A in $\mathcal{H}_{|\psi\rangle}$.

$$\langle \psi | \beta_k \rangle = \langle \psi | \mathbb{1}_{\mathcal{H}_{|\psi\rangle}} | \beta_k \rangle \quad (\text{A.1})$$

$$\begin{aligned}
&= \langle \psi | \sum_{j^\pm} |\alpha_j^\pm\rangle \langle \alpha_j^\pm | \beta_k \rangle \\
&= 2\langle \psi | \beta_k \rangle \sum_{j^\pm} \frac{|\langle \alpha_j^\pm | \psi \rangle|^2}{1 - e^{i(\beta_k \mp \alpha_j)}} \\
\frac{1}{2} &= \sum_{j^\pm} \frac{|\langle \alpha_j^\pm | \psi \rangle|^2}{1 - e^{i(\beta_k \mp \alpha_j)}}
\end{aligned}$$

$$0 = \sum_{j^\pm} |\langle \alpha_j^\pm | \psi \rangle|^2 \cot\left(\frac{\beta_k \mp \alpha_j}{2}\right) \quad (\text{A.2})$$

where in the last line we use the identity $(1 - e^{i\chi})^{-1} = \frac{1}{2} + \frac{i}{2} \cot(\frac{\chi}{2})$.

As we increase the eigenphase β_k in Eq. A.2, the right-hand side decreases monotonically except when $\beta_k = \pm\alpha_j \pmod{2\pi}$ for some α_j , where the sum jumps from $-\infty$ to $+\infty$. Thus, the right-hand side has exactly one root strictly in between each consecutive eigenphase of A in $\mathcal{H}_{|\psi\rangle}$. \square

Proof of Lemma 4

First, consider the case where $\mathcal{H}_{|\psi\rangle}$ contains a one-dimensional (+1)-eigenspace of A , which occurs just in case $|\psi\rangle$ overlaps the (+1)-eigenspace of A . Then by Lemma 14, A' does not have any (+1)-eigenvector in $\mathcal{H}_{|\psi\rangle}$. Outside of $\mathcal{H}_{|\psi\rangle}$, A and A' both have a

(+1)-eigenspace of dimension $d_+ - 1$. In the full space, A' thus has a (+1)-eigenspace of dimension $d_+ - 1$.

Second, consider the case where $\mathcal{H}_{|\psi\rangle}$ does not contain any (+1)-eigenspace of A , which occurs just in case $|\psi\rangle$ does not overlap the (+1)-eigenspace of A . Then there must be a unique eigenphase of A' on the unit circle strictly in between the smallest positive and negative eigenphases of A . Since A' is real, its eigenphases come in positive/negative pairs, so this unique eigenphase of A' must be its own negative and hence equals zero. This zero eigenphase corresponds to a single (+1)-eigenvector of A' in $\mathcal{H}_{|\psi\rangle}$. Outside $\mathcal{H}_{|\psi\rangle}$, A and A' both have a (+1)-eigenspace of dimension d_+ . In the full space, A' thus has a (+1)-eigenspace of dimension $d_+ + 1$. \square

An equivalent statement for the (-1)-eigenspace proceeds by applying the above arguments to $-A$ and $-A'$, but we do not use it in this thesis.

Appendix B

General Real Unitaries

Given a real unitary W composed of c two-dimensional rotations, $d - c - 1$ reflections, and a unique $+1$ eigenvector (so that W acts in a $(d + c)$ -dimensional space), we show how to construct the operators T , S , and D , effectively performing Szegedy's construction in reverse.

Using the complex conjugate root theorem, we denote eigenvalues of W as $\alpha_0 = +1$ (unique), the c conjugate pairs $e^{\pm i\alpha_j}$ for $0 < \alpha_0 < j \leq c < \pi$, and the reflections $\alpha_{c < j < d-1} = -1$. These have associated eigenvectors $|V_0\rangle$, the complex conjugate states $|V_{0 < j \leq c}^\pm\rangle$, and the reflected states $|V_{c < j \leq d}\rangle$. We can thus write W as

$$W = |V_0\rangle\langle V_0| + \sum_{j=1}^c (e^{i\alpha_j} |V_j^+\rangle\langle V_j^+| + e^{-i\alpha_j} |V_j^-\rangle\langle V_j^-|) - \sum_{j=c+1}^{d-1} |V_j\rangle\langle V_j|. \quad (\text{B.1})$$

We define T and S as follows,

$$T = |V_0\rangle\langle 0| + \frac{1}{\sqrt{2}} \sum_{j=1}^c (|V_j^+\rangle + |V_j^-\rangle)\langle j| + \sum_{j=c+1}^{d-1} |V_j\rangle\langle j| \quad (\text{B.2})$$

$$S = 2|V_0\rangle\langle V_0| + \sum_{j=1}^c (e^{i\alpha_j/2} |V_j^+\rangle + e^{-i\alpha_j/2} |V_j^-\rangle)(e^{-i\alpha_j/2} \langle V_j^+| + e^{i\alpha_j/2} \langle V_j^-|) - \mathbb{1}. \quad (\text{B.3})$$

Next we show that, using these definitions, $W = S(2TT^\dagger - \mathbb{1})$,

$$\begin{aligned} S(2TT^\dagger - \mathbb{1})|V_0\rangle &= S|V_0\rangle \\ &= |V_0\rangle \\ S(2TT^\dagger - \mathbb{1})|V_{0 < j \leq c}^\pm\rangle &= S|V_j^\mp\rangle \\ &= e^{\pm i\alpha_j/2} (e^{i\alpha_j/2} |V_j^+\rangle + e^{-i\alpha_j/2} |V_j^-\rangle) - |V_j^\mp\rangle \\ &= e^{\pm i\alpha_j} |V_j^\pm\rangle \end{aligned}$$

$$\begin{aligned}
S(2TT^\dagger - \mathbb{1})|V_{c < j < d}\rangle &= S|V_j\rangle \\
&= -|V_j\rangle.
\end{aligned}$$

Next, we derive the d -dimensional operator D from S and T as

$$\begin{aligned}
D &= T^\dagger S T \\
&= T^\dagger \left(2|V_0\rangle\langle 0| + \sqrt{2} \sum_{j=1}^d (e^{i\alpha_j/2}|V_j^+\rangle + e^{-i\alpha_j/2}|V_j^-\rangle) \cos\left(\frac{\alpha_j}{2}\right) - T \right) \\
&= 2|0\rangle\langle 0| + 2 \sum_{j=1}^c \cos^2\left(\frac{\alpha_j}{2}\right) |j\rangle\langle j| - \mathbb{1} \\
&= |0\rangle\langle 0| + \sum_{j=1}^c \cos(\alpha_j) |j\rangle\langle j| - \sum_{j=c+1}^{d-1} |j\rangle\langle j|. \tag{B.4}
\end{aligned}$$

Next, let $|\rho'\rangle$ be a state that is not necessarily normalized and that satisfies $\langle 0|\rho'\rangle = 1$.

Then define

$$|x'\rangle = (D - \mathbb{1})^+ (|\rho'\rangle - |0\rangle) \tag{B.5}$$

where we use the pseudo-inverse of $D - \mathbb{1}$, i.e.

$$(D - \mathbb{1})^+ = \sum_{j=1}^c (\cos(\alpha_j) - 1)^{-1} |j\rangle\langle j| - \frac{1}{2} \sum_{j=c+1}^{d-1} |j\rangle\langle j|.$$

Since $|\rho'\rangle - |0\rangle$ and $|x'\rangle$ have no overlap with $|0\rangle$, it follows that

$$\begin{aligned}
(D - \mathbb{1})|x'\rangle &= |\rho'\rangle - |0\rangle \\
D|x'\rangle &= |x'\rangle + |\rho'\rangle - |0\rangle.
\end{aligned}$$

Next, we fix an alternative orthonormal basis $\{|k_P\rangle, k \in [N]\}$ of the space spanned by $\{|j\rangle, j \in [N]\}$, such that $\langle 0|k_P\rangle > 0 \forall k \in [N]$. The states $|k_P\rangle$ then play the role of vertices.

Accordingly, we the elements

$$\sqrt{\pi_k} = \langle k_P | 0 \rangle$$

$$\tau_k = \sqrt{\pi_k} \langle k_P | \rho' \rangle$$

$$x_k = \sqrt{\pi_k} \langle k_P | x' \rangle$$

$$P = \sum_{k=0}^{d-1} \sqrt{\pi_k} |k_P\rangle \langle k_P| D \sum_{\ell=0}^{d-1} \sqrt{\pi_\ell}^{-1} |\ell_P\rangle \langle \ell_P|.$$

Using these elements, we can make the identifications

$$|0\rangle = \sqrt{\vec{\pi}} \tag{B.6}$$

$$|\rho'\rangle = \frac{\vec{\tau}}{\sqrt{\vec{\pi}}} \tag{B.7}$$

$$|x'\rangle = \frac{\vec{x}}{\sqrt{\vec{\pi}}}. \tag{B.8}$$